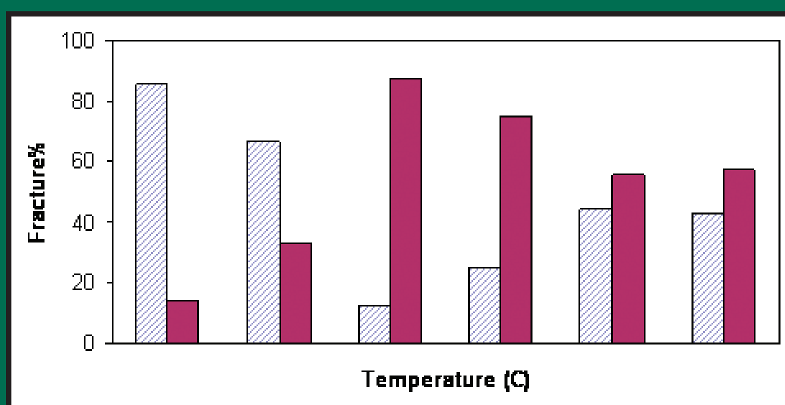

Temperature Effect on Impact Performance Advanced High-Strength Steel (AHSS) Welds

A/S P Auto/Steel Partnership

www.a-sp.org

A/SP Joining Technologies Committee Report

TEMPERATURE EFFECT ON IMPACT PERFORMANCE OF ADVANCED HIGH STRENGTH STEEL (AHSS) WELDS

Project Leader

Bipin B. Patel

DaimlerChrysler Corporation

Testing Personnel

Amir R. Shayan

Xiao Su

Supervised by

Professor Hongyan Zhang

Materials Joining Lab

Mechanical, Industrial and Manufacturing Eng. Dept

The University of Toledo

Toledo, OH

Executive Summary

This project was conducted in order to study the effect of temperatures on the behavior of AHSS resistance spot welds, under impact loading conditions.

Background

The Auto/Steel Partnership Joining Technologies Committee has conducted various projects on weldability, quality assessment, and other aspects of welding of AHSS. The performance data has only been generated under ambient temperature conditions and has not considered effects, if any, of extreme temperatures on performance. Preliminary studies conducted by the University of Toledo and General Motors with regards to "The effect of low temperatures on impact performance of resistance welded AHSS specimens" have been inconclusive and sometimes contradictory. This study was conducted to provide a better understanding of the effects of extreme cold/hot weather conditions of resistance spot welded joints.

Testing Conditions

Temperature range: -60^{o}C ~ +55^{o}C

Testing speeds: 5 mph and 15 mph

Material combinations:

C1: DP780-2.0mm to DP780-1.0mm

C2: DP780-2.0mm to DP780-1.2.0mm

C3: DP780-2.0mm to DP780-1.4mm

C4: DP590-1.0mm to Mild Steel-1.0mm

C5: DP590-1.0mm to Mild Steel-2.0mm

Methodology

Five different material stack-ups consistent with the A/SP "Roadmap" for future application of AHSS have been resistance spot welded for this project. Weld schedules used were the optimized weld schedules previously developed in support of the Lightweight Front End Structure (LWFS) project. The welded specimens were subjected to low temperatures through the use of liquid nitrogen, dry ice, or ice in a cooling chamber and to higher temperatures with the use of infrared or other type of heaters. Six different temperature conditions between ~ -60°C to ~ +55°C (-76° F to 131°F) and 5 replicates to be impact tested at two different impact speeds (5 and 15 mph) were considered for this test. A fast response digital thermometer with a sensing arm was used to measure the surface temperature of the weld immediately before testing. Impact testing was conducted using the double pendulum impact tester at the University of Toledo.

Major Findings

The experimental results obtained indicate that temperature does not affect have a significant impact performance of the resistance spot welds of advanced high strength steel and mild steel material, and the impact speeds and materials combinations have larger effects. The major findings are listed in the following.

Temperature Effect

1. Energy curves for all the material combinations studied do not show a significant effect of temperature on performance. Plots of data are relatively flat with the exception of C5. C5 shows an increase in toughness in the temperature range -30°C. to 0°C and then remains fairly stable at higher temperature range.
2. C1, C2, and C3 combinations tested at 15 mph impact speed show that the button pulled tend to remain on the thinner sheet at lower temperature, and on the thicker sheet at a higher temperature.
3. C1, C2 and C3 combinations tested at 15 mph show that the energy trend drops as temperature increases from 30°C to 55°C.

Impact Speed Effect

4. Most of the C1, C2, C3 and C5 combinations tested at 5 mph show that the welds did not separate regardless of temperature.
5. All combinations separated when the impact speed was raised to 15mph.

Material Effect

6. Large number of specimens in C1 showed expulsion and in C3 with interfacial fracture mode. The weld specimens w/expulsion and interfacial fracture modes showed lower energy than those w/o expulsion and interfacial fracture.

7. When similar sheet thicknesses of AHSS and mild steel are welded, the button pulled tend to remain on the sheet with higher yield strength. When thinner higher strength material is welded to thicker mild steel, the button pulled tend to remain on the thicker sheet with the higher stiffness.

TABLE OF CONTENTS

LIST OF TABLES

LIST OF FIGURES

ABSTRACT

This study has been conducted to quantify the effect of temperature on impact properties of resistance spot-welded advanced high strength steel combinations, consistent with the A/SP "Roadmap" for future application of AHSS. Weld schedules used were the optimized weld schedules previously developed in support of the Lightweight Front End Structure (LWFS) project.

The comparative study has been conducted in the temperature range of ~ -60^{o}C to high ~ +55^{o}C. The impact speeds on joint performance of resistance spot-welded AHSS and mild steel have been chosen at two different levels of 5 and 15mph. The results of this study are intended to help optimal design of automotive structures using AHSS.

In chapter I of the report, the impact testing methods and instrumentations are discussed. The test equipment includes mechanical and electrical components with built-in software Labview® to acquire and present the test data.

Chapter II presents the impact test results at impact speeds of 5 and 15mph. Statistical analysis has been used to present the energy of different material combinations at 15 mph. Also, the expulsion and interfacial fracture modes results have been included in this chapter.

In Chapter III, test results are discussed and final conclusions are stated.

Nomenclatures

Abbreviations:

AHSS: Advanced High Strength Steels

R: Replicate

C: Stack-up combination

C1: DP780-2.0mm to DP780-1.0mm

C2: DP780-2.0mm to DP780-1.2.0mm

C3: DP780-2.0mm to DP780-1.4mm

C4: DP590-1.0mm to Mild Steel-1.0mm

C5: DP590-1.0mm to Mild Steel-2.0mm

RT: Room temperature

X: Unbroken specimen

O: Broken specimen

BP: Button pulled

FIF: Full interfacial fracture

CBS: Complete button separation

Quantities:

θ_o: desired angle of loading (degree)

θ_A: maximum angle of swing of the active pendulums after impact (degree)

θ_B: maximum angle of swing of the passive pendulums after impact (degree)

$E_{Specimen}$: energy consumed by the welded specimen (J)

M_A: mass of the active pendulum (kg)

M_B: mass of the passive pendulum (kg)

L_A: arm length of the active pendulum from mass center to pivotal point (m)

L_B: arm length of the passive pendulum from mass center to pivotal point (m)

g: gravitational acceleration (m/s^2)

E_{Error}: energy consumed by the system, i.e. friction and aerodynamic drag (J)

μ: sample mean

σ: pooled standard deviation

Q_1: lower quartile

Q_2: upper quartile

IQ: interquartile range, the difference of (Q_2 - Q_1)

M: bending moment (Nm)

I: area moment of inertia (m^4)

b: width (mm)

h: thickness of sheet (mm)

σ_o: maximum stress near the sheet surface (MPa)

$\sigma_{o, mild}$: maximum stress near the mild steel sheet surface (MPa)

$\sigma_{o,DP}$: maximum stress near the DP590 sheet surface (MPa)

σ_{mild}: yield strength of the mild steel (MPa)

σ_{DP}: yield strength of DP590 steel (MPa)

h_{mild}: thickness of the mild steel (mm)

h_{DP}: thickness of the DP590 sheet (mm)

I_{mild}: moment of inertia of the mild steel (m^4)

I_{DP}: area moment of inertia of the DP590 sheet (m^4)

P_{ave}: average peak load (kN)

E_{ave}: average energy (J)

D_1: first reading of weld button size (mm)

D_2: second reading of weld button size (mm)

D_{ave}: average weld button size (mm)

Chapter I

Testing Procedure and Instrumentation

1.1 Introduction

While extensive static tests have been performed on resistance spot welds, elaborate machines, fixtures and instrumentation have been developed and refined over time, impact testing of resistance spot welds is relatively new. The challenge in impact testing of resistance spot welds lies in evolving a methodology which can accurately evaluate the energy absorbed by a resistance spot weldment over a wide range of materials. To meet this challenge an impact tester was designed and developed at the University of Michigan, Ann Arbor by Zhang et al [1] and refined at the University of Toledo. The impact testing methodology developed and applied on this machine was proven to provide accurate and reliable results. This machine is able to test materials of low strength such as low carbon steels (ultimate tensile strength <280 MPa), as well as advanced high strength steels (AHSS) such as martensitic steel with an ultimate tensile strength of 1355 MPa.

1.2 Testing Principle

The impact tester works on the principle of conservation of energy. The input energy is the potential energy of the active pendulum. The potential energy is dissipated in the following forms during a test:

1. The kinetic energies of the active and passive pendulums.
2. Friction losses in the machine which include the mechanical friction and fluid friction of the moving elements with the surrounding air.
3. Energy needed to fracture the specimen.

The first two forms of energies are known quantities and the third can be calculated by taking an energy balance with the input potential energy.

1.3 Mechanism and Operation

The picture of the impact tester is shown in the Figure 1.1. It uses pendulums for input and energy measurements similar to a Charpy tester. However, there are two pendulums on this device, unlike one pendulum on a Charpy tester.

FIGURE 1.1: The impact tester.

A photograph of the machine is shown in Figure 1.1. A schematic diagram is shown in Figure 1.2(a). The pendulum marked '*A*' in the Figure 1.2 is the active pendulum because it provides the energy, and the pendulum marked '*B*' is the passive pendulum. The impact specimen is a lap-shear specimen and it consists of two strips of given materials which are bent at the ends and welded together with some overlap. See Figure 1.3. Before testing, the Z-shaped spot welded specimen is mounted on the fixture of the machine. The specimen is mounted on pendulum B at one end and attached to the fixed machine base at the other end. The specimen is clamped at the bends at both ends to ensure secure gripping of the specimen during impact. Also, the fixture and the specimen are designed in such a way that the passive pendulum is in a vertical position after clamping of the specimen. The vertical position of the passive pendulum ensures that at the instant of impact, the passive and active pendulums are both vertical and there is a full surface contact between the impact pieces on both pendulums to transmit maximum possible energy from the active to the passive pendulum.

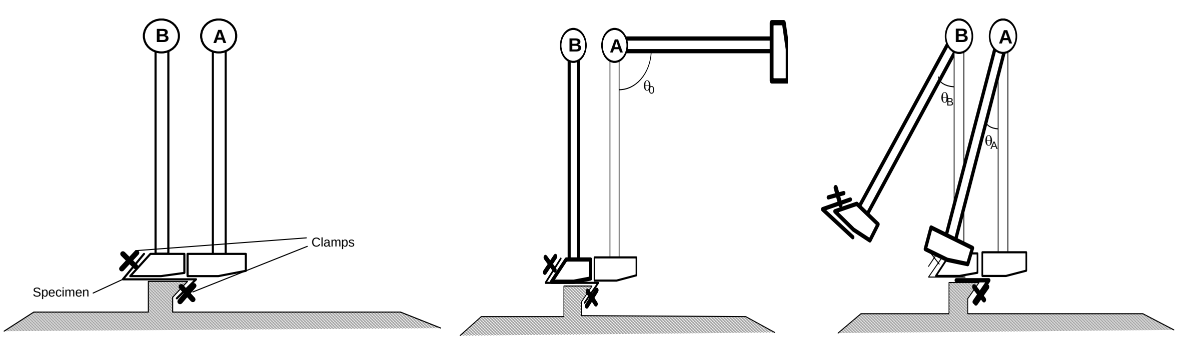

(a) ***(b)*** ***(c)***

FIGURE 1.2: Impact testing procedure: clamping the test specimen (a); before impact (b); and after impact (c).

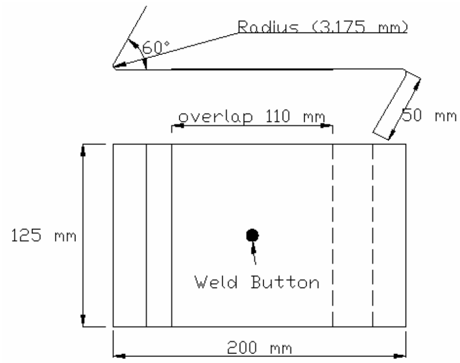

FIGURE 1.3: Impact test specimen.

Figure 1.2 illustrates the impact procedure. Before testing, the active pendulum is held at the desired angle of loading, Figure 1.2(b), θ_o (θ_o = 90° in the figure). At this stage, the system has a defined potential energy. Additional blocks (weights) can be added to the active pendulum to adjust the input energy. When the pendulum is released, its potential energy is converted into kinetic energy which reaches its maximum value at the bottommost position immediately before impact. After the impact, the struck passive pendulum moves in the impact direction and pulls the specimen apart, Figure 1.2(c). If there is enough kinetic energy, the welded specimen separated into two parts and both pendulums will continue to swing forward because of the remaining energy in the system. The maximum angles of swing of the active and passive pendulums after impact, θ_A and θ_B respectively, will be recorded by dial meters. The energy consumed by the welded specimen ($E_{Specimen}$) can be expressed as

$$E_{Specimen} = M_A\, g\, L_A \cos\theta_A - M_B\, g\, L_B\,(1-\cos\theta_B) - E_{Error} \qquad (1\text{-}1)$$

where M_A and M_B are the masses of the active and passive pendulums, respectively, L_A and L_B are the mass centers of the active and passive pendulums from their pivotal points respectively, g is the gravitational acceleration, θ_A and θ_B are the maximum swing angles of the active and passive pendulums after impact respectively, and E_{Error} is the energy consumed by the system such as friction and aerodynamic drag. After E_{Error} has been determined, the maximum angles of the pendulums are the only quantities needed to calculate the energy consumed by the specimens.

1.4 The Specification of the UT Impact Tester

The impact tester has a provision whereby the input potential energy of the active pendulum can be varied from 364 Joules to 2122 Joules by changing the angle of loading (θ_o). See Figure 1.3. This enables testing spot welds of very high strength materials which require high input potential energies to achieve fracture.

The adjustable angle of loading enables the velocity of the active pendulum at the instant of impact, which is a critical factor in impact testing, to be varied so as to achieve desired testing conditions. This makes the machine versatile in the range of materials handled, the weld geometry tested and the desired input conditions.

1.5 Instrumentation

The instrumentation plays an important role in impact testing because fracture modes involving high deformation rates like those occurring in impact testing need advanced instrumentation to capture the energy, load and the displacement responses.

In the impact tester, the impact strength of a specimen (in the form of energy) can be evaluated by recording the dial meter readings for the swing angles for both pendulums. The energy is calculated by entering the swing angle into the energy equation. This is an important advantage in terms of measurement since a direct correlation between the swing angle on the scale and energy of the pendulums is achieved without complicated mechanisms.

However, detailed information of impacting, such as impact force and its variation with time, are only derived from instruments measurement. The major difference in instrumentation from quasi-static testing is that sensors used in impact testing must have a high response rate. The deformation and force profiles are of particular interest.

On the impact tester, a system of four force sensors is used to measure the resisting force being generated in the spot weld dynamically. These sensors are strain gauge type compression load cells. Each load cell has a capacity of 25,000 lbs (111.5 kN) which is sufficient for the impact forces generated in testing high strength material. Two sensors in the front and another two sensors on the rear are mounted on the fixture that clamps the specimen. The output from each sensor is interfaced with the computer. From this output, the impact force or the peak load generated during the test is calculated.

To measure the displacement of the spot weld during fracture, a displacement sensor is mounted on the machine. It is a non-contact fiber-optic displacement sensor with a range of 17-mm. This sensor is a reflective type fiber-optic displacement transducer utilizing bundled glass fibers to transmit light to, and to receive reflections from the target surfaces. This sensor is reflectance dependent. The output voltage is proportional to the distance between the sensor tip and target surface as well as the reflectivity of the target surface. This type of sensor is commonly used in applications where the target has a reciprocating or vibratory motion parallel to the axis of the sensor. As the spot weld undergoes impact tresting, the specimen orients itself with the swing of the passive pendulum. Therefore, a measure of the deformation of the specimen is achieved by measuring the swing of the passive pendulum during impact. By placing a mirror, which acts as a reflecting surface on the passive pendulum head, the displacement can be measured by the sensor. This displacement sensor records the distance, as a function of time, between the fiber optic sensor tip and a mirror. Its characteristic of non-contact measurement is critical in impact testing. The output voltage is only proportional to the distance between sensor tip and target surface. Based on a sensor response curve; the measured voltage can be converted into the actual displacement value.

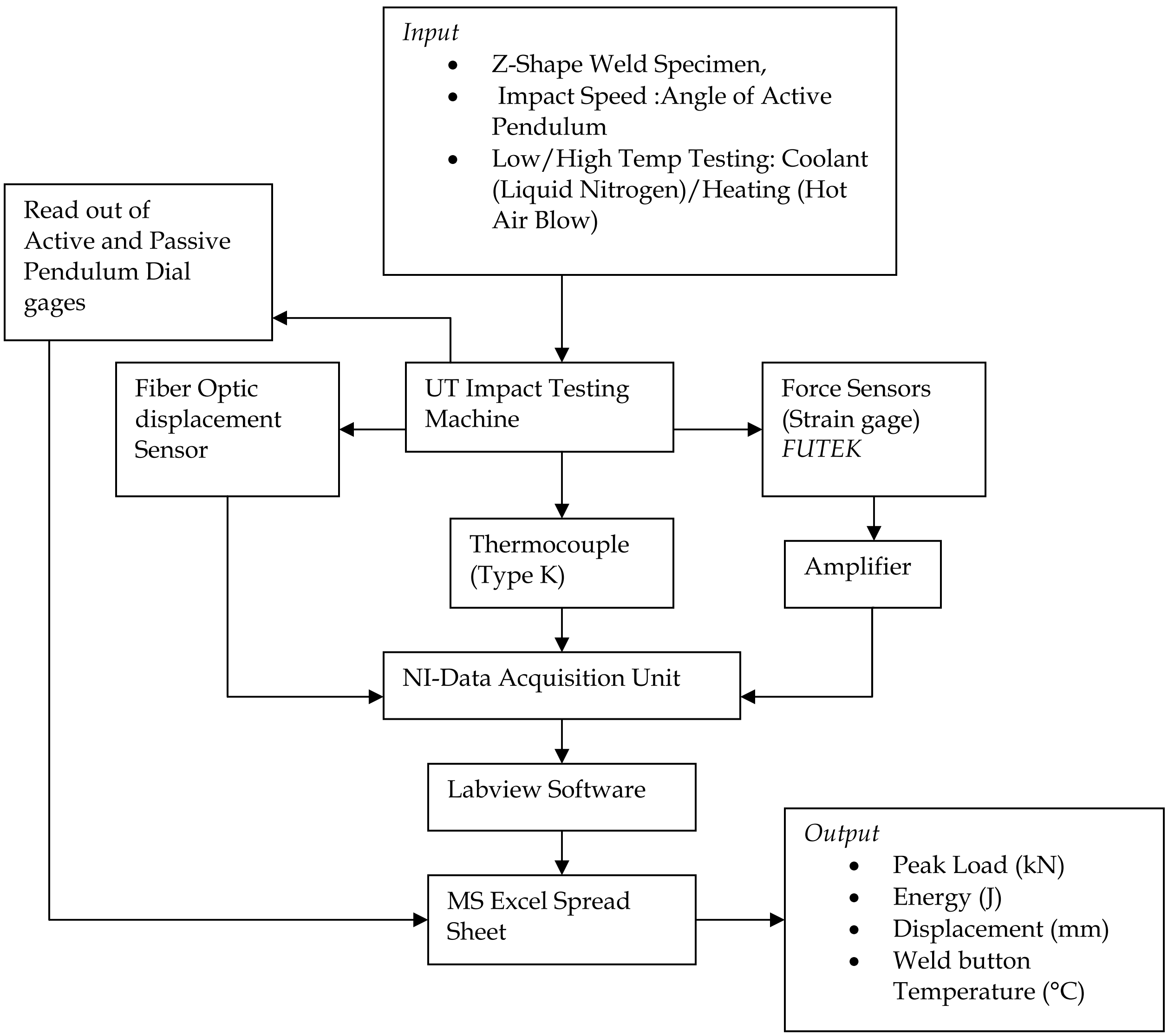

FIGURE 1.4: Schematic diagram of impact testing.

FIGURE 1.5: UT impact testing machine and cooling system.

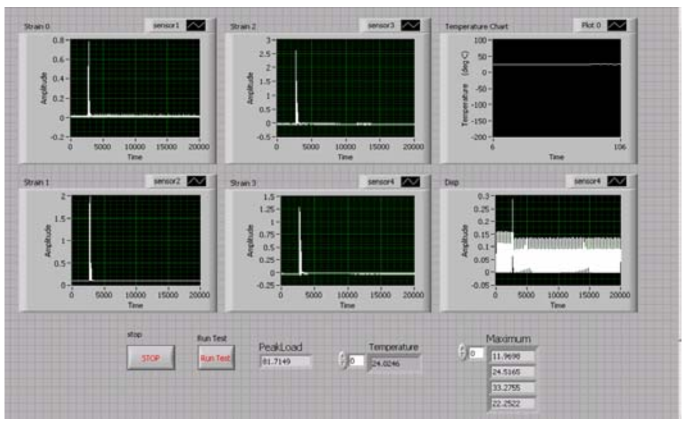

FIGURE 1.6: Labview® front panel for impact test with 4 force sensors, displacement and temperature signals.

Chapter II

Impact Test Results at 5 mph & 15 mph

2.1 Impact Tests at 5 mph

Most of the specimens, when tested at 5 mph, did not separate in the temperature range between -60°C and +55°C. However, for material combinations C3 and C4, some interesting observations could be made from the results as shown in Table 1. C3, specimens tested at lower temperatures (-60°C and -30°C) tend to break under impact. It could be estimated that there is an increase in toughness between -30°C and -15°C. Material combination C4 has more specimens broken than any other combinations. The energy for the broken specimens of C4 is plotted in Figure 2.1(a). It is apparent that there is not much difference in energy over the testing temperature range as the curve is relatively flat. A similar trend is observed in the peak load of C4, although it shows a fluctuation at -30°C, See Figure 2.1(b).

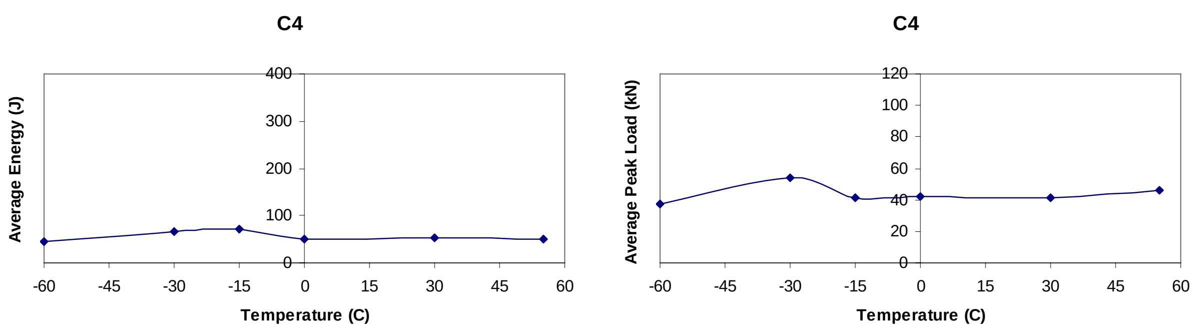

(a) *(b)*

FIGURE 2.1: Average energy (a) and peak load (b) curves of combination C4: DP590-1.0 mm to Mild Steel-1.0 mm, at 5 mph.

2.1.1 C1 (DP 780-2.0 mm to DP780-1.0 mm)

At -60°C and -30°C, the welds for the first specimen did separate and then the welds for 3 specimens tested did not separate. It was concluded that the majority of this combination can withstand the impact at this temperature range. For the rest of the temperatures, after finding that the first or second specimen withstood the impact, the testing was stopped. Specimens were expected to have higher toughness in the higher temperature range. It was concluded that for combination C1 the welds can withstand the impact at 5 mph between -60°C and +55°C.

2.1.2 C2 (DP780-2.0 mm to DP780-1.2 mm)

One specimen was tested at each temperature and none of the welds separated. Another replicate was tested at room temperature (RT) and it also withstood the impact. It was concluded that for combination C2, the welds can withstand impact at 5 mph between -60°C and +55°C.

2.1.3 C3 (DP780-2.0 mm to DP780-1.4 mm)

Most of the welds for these combinations were separated under impact between -60°C and -30°C. At -15°C, 3 out of 4 specimens did not break. At higher temperatures all the specimens withstood the impact. This combination shows an increase in toughness between -30°C and -15°C. It was concluded that for combination C3 the welds can withstand the impact at 5 mph when tested between -15°C and +55°C

2.1.4 C4 (DP590-1.0 mm to Mild Steel-1.0 mm)

This combination yielded results which were contrary to the expectations. Most of the specimens withstood the impact between -60°C and -30°C. However, welds for all of the specimens at higher temperatures did separate, except one at -15°C. This is opposite to what is normally seen in most of the steels. This could be attributed to the difference in mechanical properties of two sheet metals (DP590 and Mild Steel) at the same gage thickness.

2.1.5 C5 (DP590-1.0 mm to Mild Steel-2.0 mm)

Most of the welds for this combination withstood the impact. It was concluded that for combination C5 the welds can withstand the impact at 5 mph between -60°C and +55°C.

2.2 Outliers and box plots

Collecting the data after impact testing at 15 mph, a statistical analysis was performed to identify outliers using MINITAB. The analysis was conducted at a 95% significance level. The results are summarized in tables with outliers (judged by impact energies) marked. The data points used to present peak load are those selected for energy plots excluding outliers (in terms of energy). At least three points were used for calculating the average values. Besides measured energy and peak load for each specimen, a visual inspection of fracture mode was performed. The button size was also measured and the results are tabulated in the appendices.

Outliers are observations with values significantly different from average response or predictor values. It is important to identify outliers because they can significantly influence the model, providing potentially misleading or incorrect results. There are several methods to identify outliers. Many researchers consider an observation an outlier if it is different from the sample mean by more than twice the pooled standard deviation, i.e. $\mu \pm 2\sigma$.

Two activities are essential for characterizing a set of data:

1. Examination of the overall shape of the graphed data for important features, including symmetry and departures from assumptions.
2. Examination of the data for unusual observations that are far removed from the mass of data. These points are often referred to as outliers. Two graphical techniques for identifying outliers, scatter plots and box plots, along with an analytic procedure for detecting outliers when the distribution is normal (*Grubbs' Test*), can be used.

The box plot is a useful graphical display for describing the behavior of the data in the middle as well as at the ends of the distributions. The box plot uses the median and the lower and upper quartiles (defined as the 25th and 75th percentiles). If the lower quartile is Q_1 and the upper quartile is Q_2, then the difference (Q_2 - Q_1) is called the interquartile range or IQ [2, 3].

A box plot is constructed by drawing a box between the upper and lower quartiles with a solid line drawn across the box to locate the median. The following quantities (called fences) are needed for identifying extreme values in the tails of the distribution:

1. lower inner fence: Q_1 - 1.5*IQ
2. upper inner fence: Q_2 + 1.5*IQ
3. lower outer fence: Q_1 - 3*IQ
4. lower inner fence: Q_1 - 1.5*IQ
5. upper inner fence: Q_2 + 1.5*IQ
6. lower outer fence: Q_1 - 3*IQ
7. upper outer fence: Q_2

A point beyond an inner fence on either side is considered an outlier. A point beyond an outer fence is considered an extreme outlier [4].

2.3 Impact tests at 15 mph

Welds from all the specimens at 15 mph were separated and statistical analysis was conducted on energy results v/s temperature for all combinations. Energy curves for these combinations are relatively flat with a low sensitivity to temperature under tested conditions. C5 combination shows an increase in toughness between -30°C and 0°C and then remains fairly stable at higher temperature range.

The variation in energy for the combinations C1 and C3 can be related to existence of expulsion and interfacial fracture modes shift, which the statistical analysis is unable to distinguish. Separating these from the rest of the specimens, it has been observed that there are large differences in the amount of energy among the two groups of specimens. See Figures 2.2 and 2.6. Figure 2.13 indicates that more than half of the fractures are at the interface of two sheets, welds with expulsion and full interfacial fracture modes, and the rest are button pulled. Expulsion and Interfacial fracture mode has been observed in whole range of testing temperature, although it is less likely at the lower end of the range, i.e. -60°C. There is also a downward trend in energy observed at temperatures between +30°C to +55°C, specifically in C1, C2, and C3.

2.3.1 C1 (DP780-2.0 mm to DP780-1.0 mm)

Energy of C1 is relatively flat, with a low sensitivity to temperature under tested conditions. A large number of specimens show evidence of expulsion. Therefore, the specimens were separated into two groups: one with expulsion and one without expulsion. The plots [Figures 2.2(a) and 2.2(b)] indicate that the effect of expulsion is more significant on energy rather than the peak load. Preliminary examination of the tested specimens shows that the specimens with expulsion tend to have smaller weld buttons.

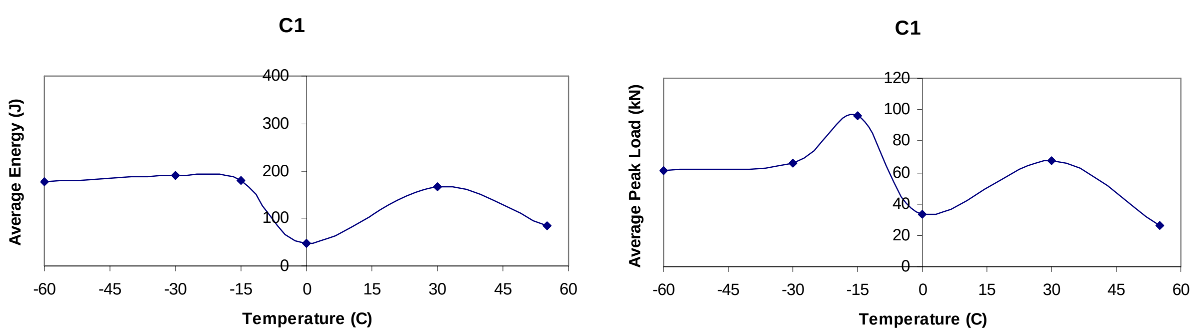

(a) *(b)*

FIGURE 2.2: Average energy (a) and peak load (b) curves combination C1: DP780-2.0 mm to DP780-1.0 mm, excluding outliers, at 15 mph.

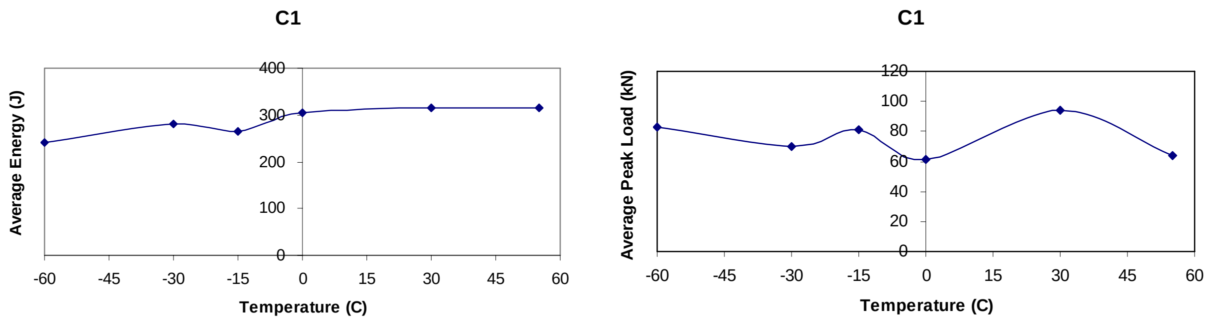

(a) *(b)*

FIGURE 2.3: Average energy (a) and peak load (b) curves of combination C1: DP780-2.0 mm to DP780-1.0 mm, without expulsion, excluding the outlier 646.66 J, at 15 mph.

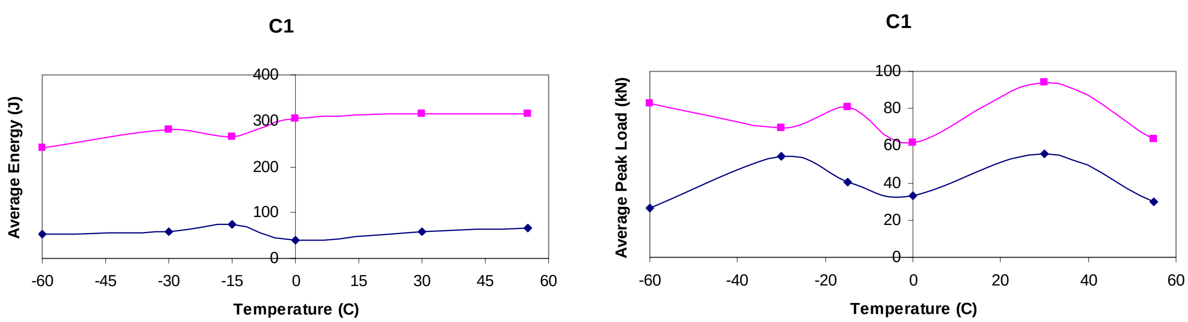

(a) *(b)*

FIGURE 2.4: Comparison of average energy (a) and peak load (b) curves of combination C1: DP780-2.0 mm to DP780-1.0 mm; w/expulsion (—◆—) and w/o expulsion (—■—), at 15 mph.

2.3.2 C2 (DP780-2.0 mm to DP780-1.2 mm)

Energy of C2 is relatively flat at low temperatures. Energy around -30°C increases and it tends to remain at the same level up to room temperature, and then it shows a drop at higher temperature from +30°C to +55°C. See Figures 2.5(a) and (b). The reason of this decrease in energy is not yet understood.

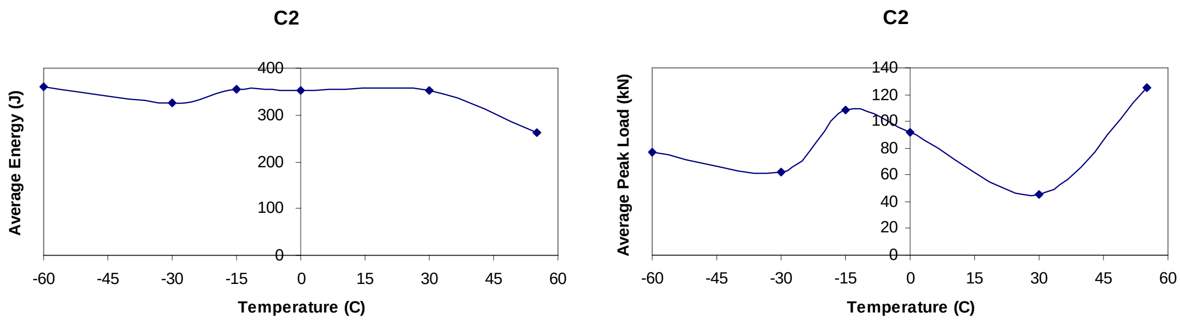

(a) *(b)*

FIGURE 2.5: Average energy (a) and peak load (b) curves of combination C2: DP780-2.0 mm to DP780-1.2 mm, excluding outliers, at 15 mph.

2.3.3 C3 (DP 780 - 2.0 mm to DP 780 - 1.4 mm)

The shape of energy curve of C3 is quite irregular. See Figures 2.6(a) and (b). Examining the specimens for the fracture mode, it shows that 45% of the specimens had button pulled and 55% of the specimens had interfacial fractures. The plot indicates that the effect of interfacial fracture is more significant on energy rather than the peak load. See Figures 2.7(a) and (b). Figure 2.8 shows interfacial fractures percentage of C3 combination at different temperatures when tested at 15 mph.

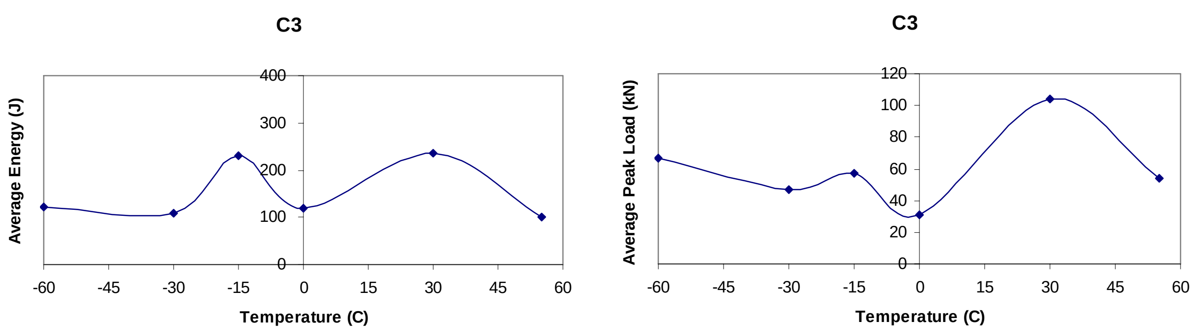

(a) *(b)*

FIGURE 2.6: Average energy (a) and peak load (b) curves of combination C3: DP780-2.0 mm to DP780-1.4mm, excluding outliers, at 15 mph.

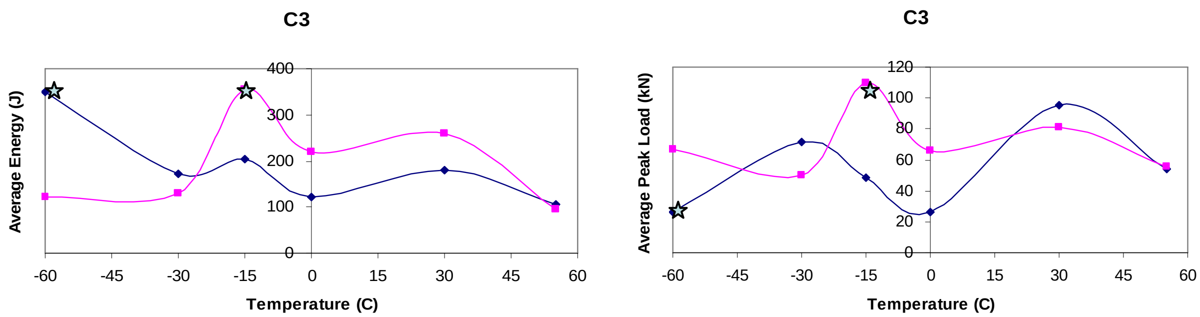

(a) *(b)*

FIGURE 2.7: Comparison of average energy (a) and peak load (b) curves for specimens with interfacial (—♦—) and button pulled (—■—) fracture of combination C3: DP780-2.0 mm to DP780-1.4mm, at 15 mph. Stars are those with a single point data.

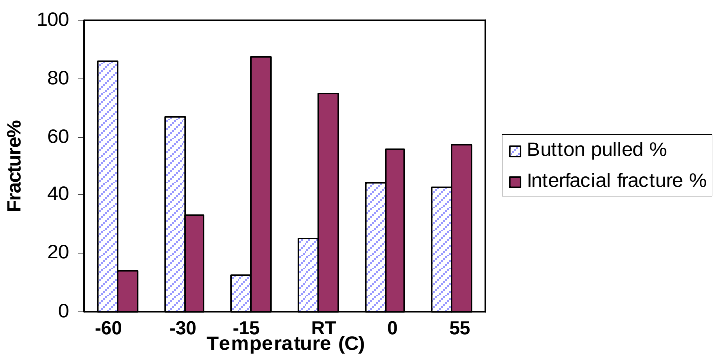

FIGURE 2.8: Interfacial fractures (%) for C3, at 15 mph.

2.3.4 C4 (DP 590-1.0 mm to Mild Steel-1.0 mm)

The energy curve of C4 is relatively flat in the tested temperature range. See Figure 2.9(a). Most of the buttons pulled tends to remain on the DP590 steel except for two cases at -60°C on the mild steel sheet. Since mild steel is a weaker material when compared to DP590, there will be a button pulled from mild steel and it will show on DP 590 steel.

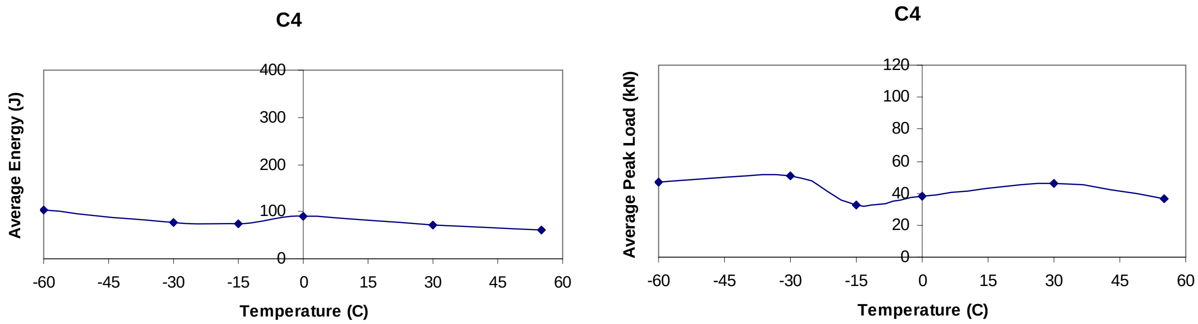

(a) *(b)*

FIGURE 2.9: Average energy (a) and peak load (b) curves of combination C4: DP590-1.0 mm to Mild Steel-1.0 mm, excluding outliers, at 15 mph.

2.3.5 C5 (DP590-1.0 mm to Mild Steel-2.0 mm)

The energy has a familiar shape and it shows an increase in toughness from lower temperatures to higher temperatures estimated around -30°C to 0°C. See Figure 2.10(a). All the buttons pulled tends to remain on the mild steel sheet, except for one specimen at -60°C, which is the thinner gage sheet in this combination. For thicker material, button pulled tends to remain on mild steel.

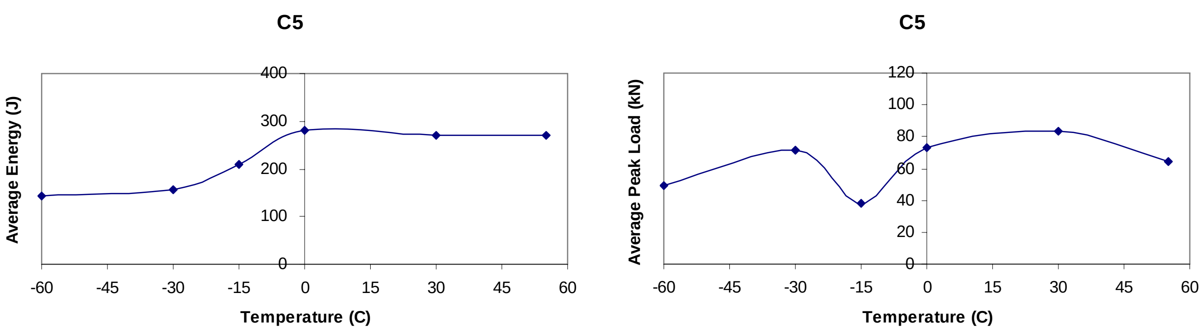

(a) *(b)*

FIGURE 2.10: Average energy (a) and peak load (b) curves of combination C5: DP590-1.0 mm to Mild Steel-2.0 mm, excluding outliers, at 15 mph.

2.4 Overall Comparison at 15 mph

Figure 2.11 represent average values of energy of all material combinations excluding outliers as determined by statistical analysis, without consideration of physical characteristics such as fracture mode or expulsion. The comparison of magnitude and trend of the energy of all material combinations are shown in Figure 2.11. Dependence of button shift on transition temperature and steel gage has been shown in Figure 2.12. An interesting observation in material stack-ups with both DP 780 steels, i.e. C1, C2, and C3, is about the interfacial fracture percentage. See Figure 2.13. As can be seen, there are no interfacial fractures in combinations C1 and C2 and all the fracture are attributed to button pulled, while 55% of fracture mode of C3 combination are related to the interfacial fractures.

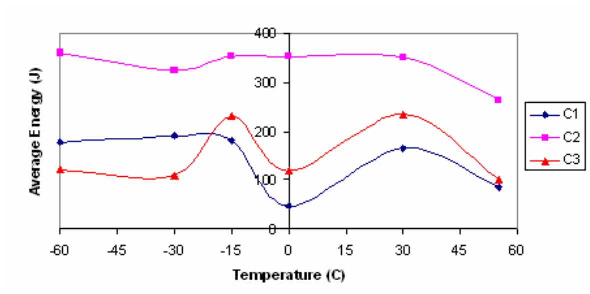

(a)

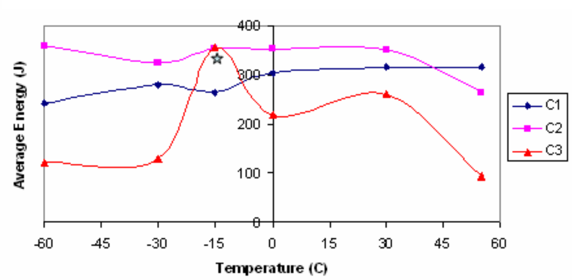

(b) ☆*Single point data only on C3*

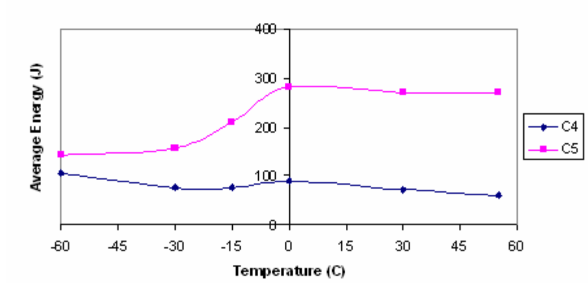

(c)

FIGURE 2.11: Average energy curves of combinations C1: DP780-2.0 mm to DP780-1.0 mm; C2: DP780-2.0 mm to DP780-1.2 mm C3: DP780-2.0 mm to DP780-1.4 mm; after statistical analysis(a); and w/ button pulled (b); C4: DP590-1.0 mm to Mild Steel-1.0 mm C5: DP590-1.0 mm to Mild Steel-2.0 mm, excluding outliers; after statistical analysis(c) , at 15 mph.

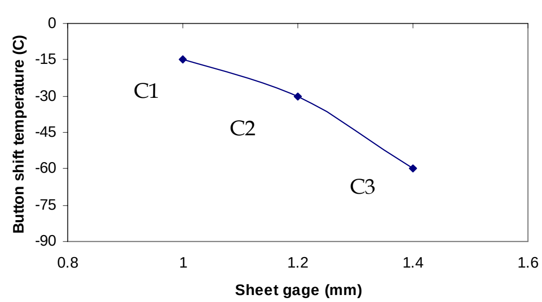

FIGURE 2.12: Dependence of fracture mode shift on transition temperature and steel gage. C1 (DP780-2.0 mm to DP780-1.0 mm), C2 (DP780-2.0 mm to DP780-1.2 mm), and C3 (DP780-2.0 mm to DP780-1.4 mm), at 15 mph.

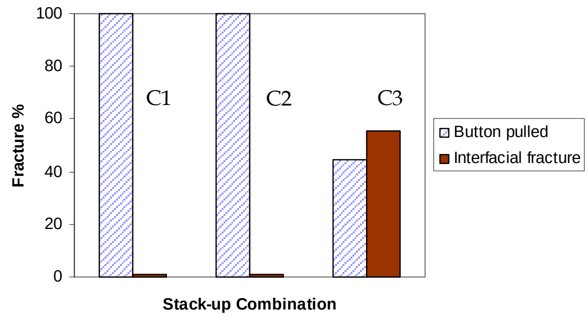

FIGURE 2.13: Interfacial fracture (%) for C1, C2, and C3, at 15 mph.

2.5 Gage effect

There is a clear gage effect when combinations C4 and C5 are compared. DP590-1.0 mm was welded to 1.0 mm mild steel in C4, and to 2.0mm mild steel in C5. Examining the fracture mode, the button pulled overwhelmingly remained on the DP590 steel sheet when it is welded to 1.0 mm mild steel sheet. The button pulled remained on the 2.0 mm mild steel sheet for all the specimens in C5. A possible explanation of this phenomenon can be drawn by considering the resistance to yielding under bending provided by the cross-sections of the sheets.

As the specimen is loaded in a tensile-shear mode, both sheets are placed under bending in the vicinity of the weld. If one of the sheets tends to bend (distort) more than the other, then the stress state in that sheet favors a deformation in which the button is separated from that sheet. Therefore, a weld button is likely to be pulled out of the sheet with less resistance to bending than that with less bending or distortion.

The tendency of distortion is related to the yielding of a sheet under a bending moment. The bending moment is the same for the two sheets, and can be expressed as

$$M = 2(I/h)\sigma_0 \qquad (2\text{-}1)$$

Where M is the bending moment, I is the moment of inertia and

$$I = (1/12)bh^3 \qquad (2\text{-}2)$$

Where b is the width, h is the thickness, and σ_0 is the maximum stress near the sheet surface, as shown in Figure 2.14. When σ_0 reaches the yield strength of the sheet, it starts to have large a distortion. Therefore, where the button resides, when pulled, largely depends on which sheet has its elastic limit exceeded at the surface. Assuming that the yield strength of the mild steel is σ_{mild} = 175 MPa, and that of DP590 is σ_{DP} = 350 MPa, DP590 is about twice as strong as the mild steel. When a weldment is under tensile-shear loading, the moments exerted on the two sheets are identical, i.e.

$$M = 2\left(I_{mild}/h_{mild}\right)\sigma_{0,mild} = 2\left(I_{DP}/h_{DP}\right)\sigma_{0,DP} \quad (2\text{-}3)$$

For C4, both sheets are 1.0 mm, so that $h_{mild} = h_{DP}$ and $I_{mild} = I_{DP}$. $\sigma_{0,mild}$ will reach σ_{mild} before $\sigma_{0,DP}$ does, and the mild steel will yield and bend before DP590 steel, creating a favorable geometry and loading mode for the weld button to be pulled out of the Mild Steel and tends to remain on the DP590 steel.

For C5, the mild steel is 2.0 mm thick, and DP590 is still 1.0 mm thick. The ratio of stresses (of DP590 steel to mild steel) is

$$\left(I_{mild}/h_{mild}\right)/\left(I_{DP}/h_{DP}\right) = \left(h_{mild}\right)^2/\left(h_{DP}\right)^2 = 2^2/1^2 = 4 \quad (2\text{-}4)$$

That is, right before yielding, $\sigma_{0,mild}/\sigma_{0,DP} = 1/4$ DP590 steel reaches its elastic limit when the mild steel is about half of its yield strength. The mild steel is twice as stiff as compared to DP590 when yield strength, thickness and geometry factors are considered. As a result, DP590 sheet tend to have a larger deformation and unfavorable stress state. Therefore, the weld button tends to remain on the stiffer 2.0 mm mild steel.

If this mathematical explanation is correct, the button pulled randomly would tend to remain on either DP590 or mild steel sheets. This could be observed when the mild steel has a thickness which makes $\left(h_{mild}\right)^2/\left(h_{DP}\right)^2 = 2$ e.g. for 1.0 mm DP590, the thickness of mild steel would be 1.4 mm.

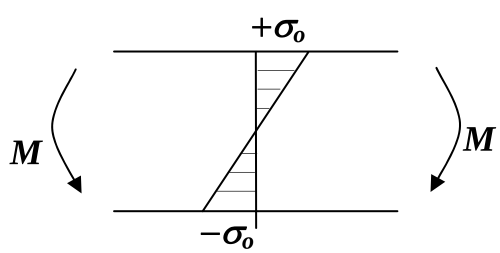

FIGURE 2.14: Bending moment (M) and maximum stress (σ_0) in steel sheets.

Chapter III

Discussion and Conclusions

3.1 Overall conclusions

The experimental results obtained indicate that temperature does not have a significant effect on impact performance of resistance spot welds of advanced high strength steel and mild steel material, and the impact speed and materials combinations have larger effects.

A) Temperature effect

1. Energy curves for all the materials combinations tested at 15 mph do not have a significant effect of temperature on impact performance. Plots of data are relatively flat with the exception of C5. C5 shows an increase in toughness in the temperature range -30°C to 0°C and then remains fairly stable at higher temperature range.
2. C1, C2, and C3 combinations tested at 15 mph impact speed show that the button pulled tend to remain on the thinner sheet at lower temperature, and on the thicker sheet at a higher temperature.
3. C1, C2 and C3 combinations tested at 15 mph show that the energy trend drops as temperature increases from +30° C to +55°C.

B) Impact speed effect

1. Most of the C1, C2, C3 and C5 combinations tested at impact speed of 5 mph show that the welds did not separate regardless of temperature
2. All material combinations separated when the impact speed was raised to 15 mph.

C) Material effect

1. Large number of specimens in C1 showed expulsion and in C3 with interfacial fracture mode. The weld specimens w/expulsion and interfacial fracture modes showed lower energy than those w/o expulsion and without interfacial fracture mode.
2. When similar sheet thicknesses were welded, the button pulled tends to remain on the sheet with higher yield strength.
3. When thinner sheet higher strength steel is welded to thicker mild steel, the button pulled tends to remain on the thicker mild steel sheet with the higher stiffness.

3.2 Detailed summary of conclusions

The major findings are summarized as follows:

1. Material combinations C1, C2, and C5 can withstand impact at 5 mph (weld remained intact).
2. There was a distinct transition in fracture mode for combination C3 at test temperature of -15ºC. Most of the welds, when tested below -15°C had button pulled and welds tested at and above -15°C did not separate when tested at 5 mph.
3. Almost all combinations did not separate except combination C4 at 5 mph impact. The response of C4 to impact sways in the temperature range between -30°C and -15°C. The behavior of C4 requires further investigation.
4. Material combination C1 show a large number of specimens with expulsion when tested at 15 mph. There is no significant number of specimens having expulsion in any other combinations. The specimens with expulsion show lower energy and a lower peak load in the entire testing temperature range than those without expulsion.
5. Material combination C3 show a large number of specimens with interfacial fracture mode when tested at 15 mph. There is no significant number of specimens having interfacial fracture mode in any other combinations. The specimens with interfacial fracture mode show lower energy and a lower peak load in the entire testing temperature range than those without interfacial fracture mode.
6. Material combination C5 shows an increase in toughness in the temperature range -30°C to 0°C and then remains fairly stable at higher temperatures when tested at 15 mph.
7. An examination of the fracture surfaces of the tested combinations C1, C2, and C3 at 15 mph shows that the fracture mode depends on both material combination and testing temperature. At low temperature, button pulled tends to remain on the thinner (relatively compliant and less toughness) sheet, and they are likely to remain on the thicker sheet at a higher temperature. There is a transition temperature for the weld buttons to shift from the thin sheet to the thick one, and such temperature goes down as the thin sheet gets thicker.
8. When 1 mm mild steel is welded to 1.0 mm DP590 (C4) the button pulled tends to remain on the sheet with higher yield strength (DP590). When 1.0 mm DP590 is welded to the 2.0-mm mild steel (C5) then the pulled button tends to remain on the thicker sheet (of higher stiffness). A simple analytical analysis demonstrates the relationship between the location of the pulled button to a sheet's resistance to bending which is a function of both sheet thickness and yield strength.

3.3 Further studies

It is recommended to conduct further studies with regards to "Effect of Weld Indentation on the Impact Performance of Advanced High Strength Steel".

References

1. Zhang, H., Zhou, M. and Hu, S. J., 2000, "Impact strength measurement of spot welds," Accepted by the Proceedings of Mechanical Engineers Part B: Journal of Engineering Manufacture, pp. 403-414.
2. Minitab ™ Release 14 Help Desk, 2003.
3. Design and Analysis of Experiments, Montgomery D.C., Wiley 5th Edition.
4. http://www.itl.nist.gov/div898/handbook/prc/section1/prc16.htm.
5. Shayan A R, Xiao S, Zhang H, Patel B, Temperatures effects on impact performance of AHSS of welds, Sheet Metal Welding Conference XII, May 2006 Detroit MI, [submitted Sept. 2005].
6. Specification for Automotive Weld Quality- Resistance Spot Welding of Steel, AWS D8.1M:200X WD-1.

Appendix A: Fracture modes

Fracture modes observed on tested specimens according to AWS standard [6]

FIGURE A.1: Full interfacial fracture

FIGURE A.2: Button pulled

Appendix B: Impact test results at 5 mph

TABLE B.1: Test results for combinations C1 through C5 at 5 mph.

Material combination	Replication	Temperature (°C)					
		-60	-30	-15	0	RT[†]	55
C1: DP780-2.0mm to DP780-1.0mm	R1	O	O	X	X	X	X
	R2	X	X			X	X
	R3	X	X				
	R4	X	X				
C2: DP780-2.0mm to DP780-1.2.0mm	R1	X	X	X	X	X	X
	R2					X	
C3: DP780-2.0mm to DP780-1.4mm	R1	X	O	O	X	X	X
	R2	O	O	X		X	
	R3	O	O	X			
	R4	O		X			
C4: DP590-1.0mm to Mild Steel - 1.0mm	R1	O	X	X	O	O	O
	R2	O	X	O	O	O	O
	R3	X	O	O	O	O	O
	R4	X	X	O			O
	R5	X	O	O			
C5: DP590-1.0mm to Mild Steel-2.0mm	R1	X	X	X	X	X	X
	R2	O	X		X	O	X
	R3	O	X			O	
	R4	X				X	
	R5	X				X	

O = Broken; X = Unbroken

TABLE B.2: Combination C1 (DP780-2.0mm to DP780-1.0mm) impact test results at various temperatures.

	Specimen	Temp. (°C)	Energy (J)	Peak Load (kN)	Test Result	Fracture Mode[6]	Button Separation		Comments
						AWS Standard	from	on	
1	06-IM-01	-60	75.36	57.85	O	BP	A	B	
2	08-IM-01	-60	*	*	X				No visible deformation, Expulsion
3	09-IM-01	-60	*	*	X				No visible deformation, Expulsion
4	12-IM-01	-60	*	50.18	X				No visible deformation
5	04-IM-01	-30	52.39	45.54	O	BP	B	A	Expulsion
6	07-IM-01	-30	*	*	X				No visible deformation
7	13-IM-01	-30	*	36.79	X				No visible deformation
8	14-IM-01	-30	*	40.98	X				No visible deformation
9	11-IM-01	-15	*	51.51	X				No visible deformation
10	05-IM-01	0	*	*	X				No visible deformation, Expulsion
11	02-IM-01	RT	*	*	X				Very small rotation on both sides
12	01-IM-01	RT	*	*	X				slight rotation on both side
13	03-IM-01	48	*	*	X				No visible deformation, Expulsion
14	10-IM-01	55	*	26.21	X				Very small rotation on both sides

DP780-1mm Sheet Clamped on Passive Pendulum.
X: Unbroken specimen; O: Broken specimen
BP: Button pulled; A: DP780-2.0mm; B: DP780-1mm

TABLE B.3: Combination C2 (DP780-2.0mm to DP780-1.2.0mm) impact test results at various temperatures.

	Specimen	Temp. (°C)	Energy (J)	Peak Load (kN)	Test Result	Comments
1	03-IM-02	-60	*	*	X	No visible deformation
2	05-IM-02	-30	*	44.70	X	No visible deformation
3	06-IM-02	0	*	*	X	No visible deformation
4	07-IM-02	0	*	36.66	X	No visible deformation
5	02-IM-02	-15	*	*	X	No visible deformation
6	01-IM-02	RT	*	*	X	No visible deformation
7	04-IM-02	55	*	23.89	X	No visible deformation

DP780-1.2.0mm Sheet Clamped on Passive Pendulum.

X: Unbroken specimen; O: Broken specimen

TABLE B.4: Combination C3 (DP780-2.0mm to DP780-1.4mm) impact test results at various temperatures.

	Specimen	Temp. (°C)	Energy (J)	Peak Load (kN)	Test Result	Fracture Mode[6]	Button Separation		Comments
						AWS Standard	from	on	
1	02-IM-03	-60	*	50.90	X				No visible deformation
2	10-IM-03	-60	33.54	16.23	O				DP780-1.4mm base metal fractured all the way through from weld spot
3	11-IM-03	-60	87.23	42.84	O	BP	D	A	
4	12-IM-03	-60	55.07	39.23	O	BP	D	A	
5	03-IM-03	-30	83.82	33.83	O	BP	A	D	
6	04-IM-03	-30	89.64	30.14	O	BP	D	A	
7	05-IM-03	-30	58.98	38.66	O	BP	D	A	
8	06-IM-03	-15	73.17	23.37	O	BP	D	A	
9	07-IM-03	-15	*	36.09	X				Slight rotation on both sides
10	08-IM-03	-15	*	32.27	X				Slight rotation on both sides
11	09-IM-03	-15	*	40.61	X				No visible deformation
12	13-IM-03	0	*	39.33	X				Slight rotation on both sides
13	14-IM-03	RT	*	*	X				Slight rotation on both sides
14	15-IM-03	RT	*	64.10	X				Slight rotation on both sides
15	01-IM-03	55	*	44.31	X				Slight rotation on both sides

DP780-1.4mm Sheet Clamped on Passive Pendulum.
X: Unbroken specimen; O: Broken specimen;
BP: Button pulled; A: DP780-2.0mm; D: DP780-1.4mm

TABLE B.5: Combination C4 (DP590-1.0mm to Mild Steel-1.0mm) impact test results at various temperatures.

	Specimen	Temp. (°C)	Energy (J)	Peak Load (kN)	Test Result	Fracture Mode[6]	Button Separation		Comments
						AWS Standard	from	on	
1	04-IM-04	-60	53.80	40.91	O	BP	F	E	
2	05-IM-04	-60	38.24	34.35	O	BP	E	F	
3	23-IM-04	-60	*	51.91	X				Significant rotation on both side
4	24-IM-04	-60	*	20.14	X				Slight rotation on both side
5	25-IM-04	-60	*	13.80	X				No visible deformation on weld spot
6	06-IM-04	-30	*	*	X				Slight rotation on both side
7	07-IM-04	-30	*	*	X				Slight rotation on both side
8	13-IM-04	-30	55.92	56.30	O	BP	E	F	
9	14-IM-04	-30	*	*	X				Button pulled on mild steel sheet , but it stuck between two sheets, no displacement recorded
10	15-IM-04	-30	78.37	51.61	O	BP	E	F	
11	08-IM-04	-15	*	*	X				Slight rotation on both side
12	09-IM-04	-15	53.80	41.68	O	BP	E	F	
13	10-IM-04	-15	50.67	*	O	BP	E	F	
14	11-IM-04	-15	88.93	39.79	O	BP	E	F	
15	12-IM-04	-15	90.57	43.48	O	BP	E	F	
16	16-IM-04	0	49.54	45.60	O	BP	E	F	
17	17-IM-04	0	50.78	40.78	O	BP	E	F	
18	18-IM-04	0	47.29	41.14	O	BP	E	F	
19	01-IM-04	RT	31.69	45.68	O	BP	E	F	
20	02-IM-04	RT	75.36	*	O	BP	E	F	
21	03-IM-04	RT	48.24	37.76	O	BP	E	F	
22	19-IM-04	48	41.01	37.37	O	BP	E	F	
23	20-IM-04	55	53.80	*	O	BP	E	F	
24	21-IM-04	55	44.94	42.41	O	BP	E	F	
25	22-IM-04	55	50.78	49.15	O	BP	E	F	

Mild steel sheet clamped on Passive Pendulum.
X: Unbroken specimen; O: Broken specimen;
BP: Button pulled; E: Mild Steel-1mm; F: DP590-1mm;

TABLE B.6: Combination C5 (DP590-1.0mm to Mild Steel- 2.0mm) impact test results at various temperatures.

	Specimen	Temp. (°C)	Energy (J)	Peak Load (kN)	Test Result	Fracture Mode[6]	Button Separation		Comments
						AWS Standard	from	on	
1	13-IM-05	-60	*	39.52	X				No visible deformation
2	14-IM-05	-60	*	35.90	X				No visible deformation
3	05-IM-05	-60	*	59.51	X				Button pulled on DP590 sheet, weld button remains on mild steel sheet, a crack forms around the weld spot on mild steel sheet
4	06-IM-05	-60	*	*	X				
5	04-IM-05	-60	*	*	X				No visible deformation, a crack extends from weld spot to the surrounding base metal on mild steel sheet
6	07-IM-05	-30	*	14.41	X				No visible deformation
7	08-IM-05	-30	*	53.93	X				No visible deformation
8	09-IM-05	-30	*	38.60	X				No visible deformation
9	12-IM-05	-15	*	33.85	X				No visible deformation
10	17-IM-05	0	*	*	X				No visible deformation
11	18-IM-05	0	*	41.80	X				No visible deformation
12	01-IM-05	RT	*	*	X				Large deformation on DP590 sheet, less deformation on mild steel sheet
13	02-IM-05	RT	78.77	51.40	O	BP	F	G	
14	03-IM-05	RT	86.27	46.83	O	BP	F	G	
15	15-IM-05	RT	*	40.75	X				No visible deformation
16	16-IM-05	RT	*	40.07	X				Very slight rotation on both sides
17	10-IM-05	48	*	35.82	X				Significant rotation on both sides
18	11-IM-05	55	*	9.88	X				Significant rotation on both sides

DP590 & Mild Steel sheets clamped on Passive Pendulum.
X: Unbroken specimen; O: Broken specimen;
BP: Button pulled; F: DP590-1mm; G: Mild Steel-2.0mm

TABLE B.7: Energy and peak load of combination C4: DP590-1.0mm to Mild Steel-1.0mm.

	Specimen	Temp. (°C)	Energy (J)	E_{ave} (J)	Peak Load (kN)	P_{ave} (kN)
1	04-IM-04	-60	53.8		40.91	
2	05-IM-04	-60	38.24	46.02	34.35	37.63
3	13-IM-04	-30	55.92		56.3	
4	15-IM-04	-30	78.37	67.15	51.61	53.96
5	09-IM-04	-15	53.8		41.68	
6	12-IM-04	-15	90.57		43.48	
7	11-IM-04	-15	88.93		39.79	
8	10-IM-04	-15	50.67	70.99	*	41.65
9	16-IM-04	0	49.54		45.6	
10	17-IM-04	0	50.78		40.78	
11	18-IM-04	0	47.29	49.20	41.14	42.51
12	01-IM-04	RT	31.69		45.68	
13	03-IM-04	RT	48.24		37.76	
14	02-IM-04	RT	75.36	51.76	*	41.72
15	20-IM-04	55	53.8		*	
16	21-IM-04	55	44.94		42.41	
17	22-IM-04	55	50.78	49.84	49.15	45.78

Appendix C: Impact test results at 15 mph

TABLE C.1: Energy (J) of combination C1: DP780-2.0mm to DP780-1.0mm.

-60°C	-30°C	-15°C	0°C	RT	55°C
53.05	53.82	47.72	34.64	54.52	41.43
106.38	60.34	52.78	35.82	62.17	63.69
216.85	252.61	62.27	50.33	135.61	70.20
247.54	270.00	130.37	57.63	243.73	85.65
259.15	317.61	147.59	58.09	336.26	118.76
646.66		263.42	289.88	368.19	289.46
		292.90	317.42		323.97
		354.06			334.50

Shaded = outlier

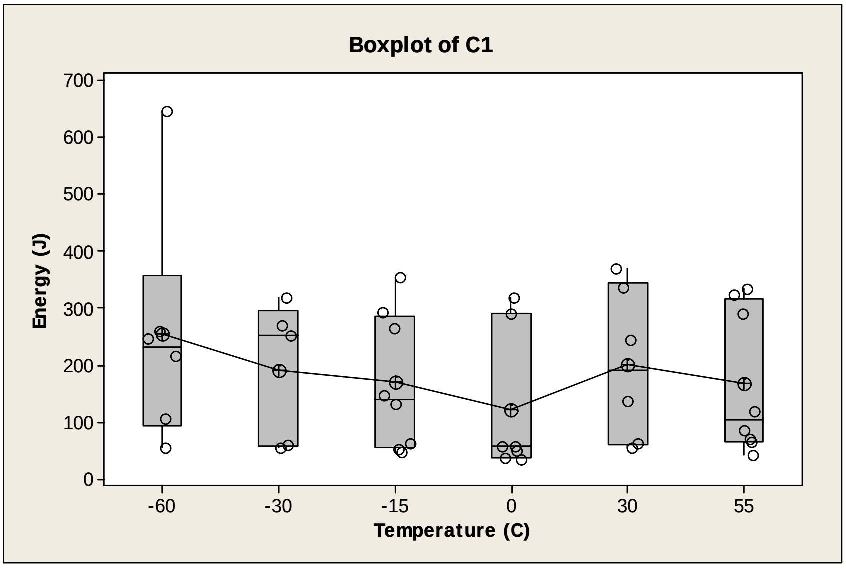

FIGURE C.1: Box plot of energy of combination C1: DP780-2.0mm to DP780-1.0mm. Mean values at each temperature are connected.

TABLE C.2: Energy (J) for specimens with & w/o expulsion of combination C1: DP780-2.0mm to DP780-1.0mm.

-60°C	-30°C	-15°C	0°C	RT	55°C
53.05	53.82	47.72	34.64	54.52	41.43
106.38	60.34	52.78	35.82	62.17	63.69
216.85	252.61	62.27	50.33	135.61	70.20
247.54	270.00	130.37	57.63	243.73	85.65
259.15	317.61	147.59	58.09	336.26	118.76
646.66		263.42	289.88	368.19	289.46
		292.90	317.42		323.97
		354.06			334.50

Shaded = w/ expulsion

TABLE C.3: Energy (J) of combination C2: DP780-2.0mm to DP780-1.2.0mm.

-60°C	-30°C	-15°C	0°C	RT	55°C
27.96	125.99	307.54	299.21	289.14	98.80
117.35	204.68	331.80	314.02	315.46	201.47
169.01	312.32	333.91	317.33	334.91	228.02
337.75	356.19	365.86	361.64	348.43	263.21
346.16	367.58	383.75	363.87	376.95	263.54
398.67	384.46	428.71	405.43	381.22	270.88
416.00			432.52	454.62	301.89
419.26					315.69
450.81					355.74

Shaded = outlier

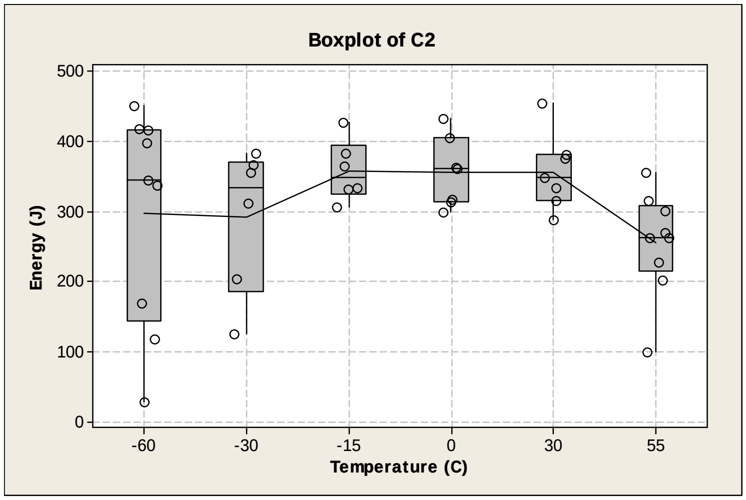

FIGURE C.2: Box plot of energy of combination C2: DP780-2.0mm to DP780-1.2.0mm. All the data points including outliers are plotted. Mean values at each temperature are connected.

TABLE C.4: Energy (J) of combination C3: DP780-2.0mm to DP780-1.4mm.

-60°C	-30°C	-15°C	0°C	RT	55°C
57.92	48.15	60.34	24.64	73.33	58.51
77.81	71.49	64.93	37.19	91.10	74.66
96.94	82.95	132.24	51.37	125.66	80.77
105.40	102.10	155.94	78.89	207.11	107.57
141.11	241.61	313.40	163.44	214.06	113.19
251.47	312.64	317.39	182.68	224.48	127.77
349.99		355.10	274.92	292.44	145.98
		379.51	358.30	312.58	
				392.58	

Shaded = outlier

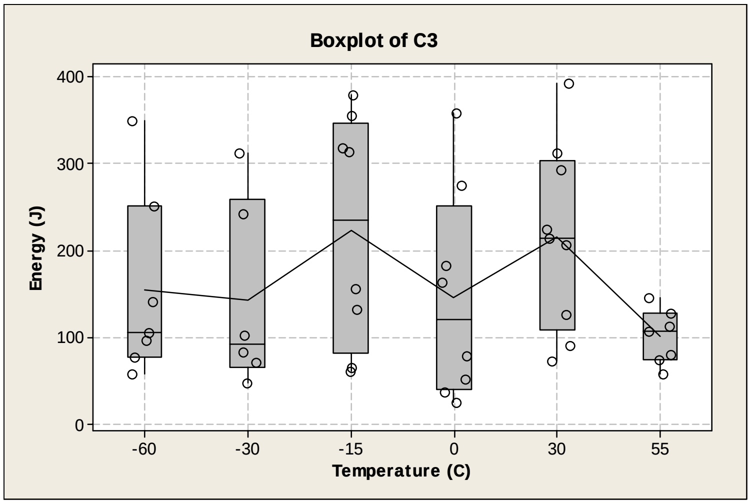

FIGURE C.3: Box plot of energy of combination C3: DP780-2.0mm to DP780-1.4mm. All the data points including outliers are plotted. Mean values at each temperature are connected.

TABLE C.5: Energy (J) for specimens with & w/o interfacial fracture of combination C3: DP780-2.0mm to DP780-1.4mm.

-60°C	-30°C	-15°C	0°C	RT	55°C
57.92	48.15	60.34	24.64	73.33	58.51
77.81	71.49	64.93	37.19	91.1	74.66
96.94	82.95	132.24	51.37	125.66	80.77
105.4	102.1	155.94	78.89	207.11	107.57
141.11	241.61	313.4	163.44	214.06	113.19
251.47	312.64	317.39	182.68	224.48	127.77
349.99		355.1	274.92	292.44	145.98
		379.51	358.3	312.58	
				392.58	

Shaded = Interfacial Fracture; Un-Shaded = Button pulled

TABLE C.6: Energy (J) of combination C4: DP590-1.0mm to Mild Steel-1.0mm.

-60°C	-30°C	-15°C	0°C	RT	55°C
60.69	54.53	59.23	66.17	50.37	0.38
68.82	55.45	69.57	73.89	57.38	41.33
97.87	97.50	84.20	106.57	60.34	51.74
108.50	100.36	88.37	110.79	118.69	90.92
122.04	176.18		135.21		128.56
123.29					

Shaded = outlier

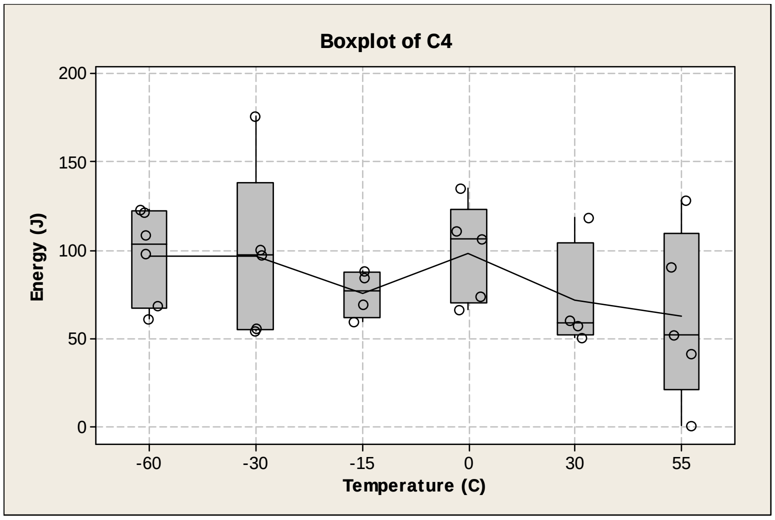

FIGURE C.4: Box plot of energy of combination C4: DP590-1.0mm to Mild Steel-1.0mm. All the data points including outliers are plotted. Mean values at each temperature are connected.

TABLE C.7: Energy (J) of combination C5: DP590-1.0mm to Mild Steel-2.0mm.

-60°C	-30°C	-15°C	0°C	RT	55°C
43.24	134.71	102.70	116.48	252.58	238.59
105.01	150.52	121.03	132.55	254.25	270.29
136.79	168.13	251.16	240.80	282.67	280.39
156.11	172.34	265.16	262.84	288.68	290.71
176.10	297.44	307.72	309.64		
			313.84		

Shaded = outlier

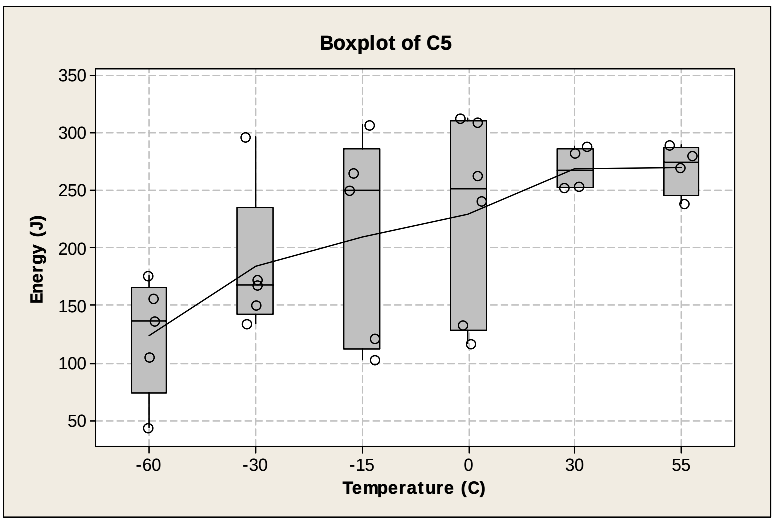

FIGURE C.5: Box plot of energy of combination C5: DP590-1.0mm to Mild Steel- 2.0mm. All the data points including outliers are plotted. Mean values at each temperature are connected.

TABLE C.8: Data Sheet of combination C1: DP780-2.0mm to DP780-1.0mm.

	Specimen	Temp.	Energy	Peak Load	Button Size(mm)			Fracture Mode[6]	Button Separation		Comments
		(ºC)	(J)	(kN)	D_1	D_2	D_{ave}	AWS Standard	from	on	
1	15-IM-01	-60	106.38		7.45	7.22	7.34	BP	A	B	
2	16-IM-01	-60	*	*	*	*	*	*	*	*	Slippage
3	17-IM-01	-60	*	*	*	*	*	*	*	*	Slippage
4	18-IM-01	-60	247.54	87.06	7.02	6.87	6.95		CBS		
5	19-IM-01	-60	216.85	113.81	6.77	7.05	6.91	BP	A	B	
6	30-IM-01	-60	646.66	29.04	6.65	6.74	6.70	BP	A	B	
7	53-IM-01	-60	53.05	26.31	6.62	6.61	6.62	BP	A	B	Expulsion
8	55-IM-01	-60	259.15	48.01	7.02	6.41	6.72	BP	A	B	
9	20-IM-01	-30	*	*	*	*	*	*	*	*	Slippage
10	31-IM-01	-30	317.61	84.97	6.64	6.48	6.56	*	A	B	
11	32-IM-01	-30	270.00	98.72	6.65	6.20	6.43		CBS		
12	33-IM-01	-30	60.34	54.62	6.31	5.22	5.77	BP	A	B	Expulsion
13	49-IM-01	-30	53.82	*	4.83	4.71	4.77	BP	B	A	Expulsion
14	58-IM-01	-30	252.61	25.21	5.14	6.01	5.58	BP	A	B	
15	45-IM-01	-15	52.78	23.61	6.29	5.37	5.83	BP	B	A	Expulsion
16	34-IM-01	-15	354.06	73.74	6.50	6.00	6.25	BP	B	A	
17	35-IM-01	-15	*	*	*	*	*	*	*	*	Slippage
18	36-IM-01	-15	292.90	43.49	6.81	6.35	6.58	*	A	B	
19	37-IM-01	-15	62.27	25.01	5.32	5.73	5.53	BP	B	A	Expulsion
20	59-IM-01	-15	130.37	81.74	5.41	5.69	5.55	BP	A	B	Expulsion
21	46-IM-01	-15	47.72	30.44	6.15	5.60	5.88	BP	B	A	Expulsion
22	50-IM-01	-15	147.59	111.53	6.63	5.71	6.17	BP	B	A	Expulsion
23	56-IM-01	-15	263.42	95.67	6.04	5.48	5.76	BP	B	A	
24	38-IM-01	0	317.42	86.45	6.27	5.94	6.11	BP	B	A	
25	39-IM-01	0	35.82	25.49	5.96	4.86	5.41	BP	B	A	Expulsion
26	40-IM-01	0	289.88	36.89	6.97	5.93	6.45	BP	B	A	
27	47-IM-01	0	58.09	47.26	6.51	6.27	6.39	BP	B	A	
28	48-IM-01	0	50.33	54.32	6.24	4.74	5.49	BP	B	A	Expulsion
29	51-IM-01	0	57.63	*	6.00	5.94	5.97	BP	B	A	
30	60-IM-01	0	34.64	5.13	4.39	5.04	4.72	BP	B	A	Expulsion
31	24-IM-01	RT	336.26	*	6.29	5.93	6.11	BP	B	A	
32	21-IM-01	RT	135.61	63.79	6.30	6.09	6.20	BP	B	A	
33	22-IM-01	RT	368.19	83.23	6.29	6.25	6.27	BP	B	A	
34	23-IM-01	RT	243.73	105.19	6.16	5.95	6.06	BP	B	A	

DP780-2.0mm Sheet clamped on passive pendulum.
BP: Button pulled; A: DP780-2.0mm; B: DP780-1.0mm; CBS: Complete Button Separation

TABLE C.8: cont'd.

	Specimen	Temp. (ºC)	Energy (J)	Peak Load (kN)	Button Size(mm)			Fracture Mode[6]	Button Separation		Comments
					D_1	D_2	D_{ave}	AWS Standard	from	on	
35	52-IM-01	RT	54.52	65.34	5.52	4.78	5.15	BP	B	A	Expulsion
36	54-IM-01	RT	62.17	36.80	5.07	5.26	5.17	BP	B	B	Expulsion
37	25-IM-01	55	289.46	84.19	6.21	5.85	6.03	BP	B	A	
38	26-IM-01	55	70.20	*	6.14	5.12	5.63	BP	B	A	Expulsion
39	27-IM-01	55	118.76	*	5.89	6.06	5.98	BP	B	A	
40	28-IM-01	55	323.97	56.02	5.90	5.90	5.90	BP	B	A	
41	29-IM-01	55	334.50	50.25	6.20	5.72	5.96	BP	B	A	
42	41-IM-01	55	63.69	28.34	5.72	4.96	5.34	BP	B	A	Expulsion
43	42-IM-01	55	41.43	37.66	6.61	4.97	5.79	BP	B	A	Expulsion
44	43-IM-01	55	*	*	*	*	*	*	*	*	Slippage
45	44-IM-01	55	85.65	23.82	6.11	5.02	5.57	BP	B	A	Expulsion

DP780-2.0mm Sheet clamped on passive pendulum.
BP: Button pulled; A: DP780-2.0mm; B: DP780-1mm

TABLE C.9: Data Sheet of combination C2: DP780-2.0mm to DP780-1.2.0mm.

	Specimen	Temp.	Energy	Peak Load	Button Size(mm)			Fracture Mode[6]	Button Separation		Comments
		(ºC)	(J)	(kN)	D_1	D_2	D_{ave}	AWS Standard	from	on	
1	08-IM-02	-60	*	*	*	*	*	*	*	*	Slippage
2	20-IM-02	-60	450.81	83.78	5.64	5.96	5.80	BP	C	A	
3	21-IM-02	-60	398.67	65.82	6.35	6.52	6.44	BP	A	C	
4	22-IM-02	-60	416.00	88.02	6.88	7.09	6.99		CBS		
5	53-IM-02	-60	117.35	48.48	6.93	5.23	6.08	BP	A	C	
6	58-IM-02	-60	27.96	50.71	6.65	6.71	6.68	BP	A	C	
7	34-IM-02	-60	337.75	73.85	6.92	7.12	7.02	BP	A	C	
8	35-IM-02	-60	419.26	62.97	6.63	6.97	6.80		CBS		
9	41-IM-02	-60	169.01	83.73	7.08	7.07	7.08		CBS		
10	42-IM-02	-60	346.16	92.35	6.82	7.14	6.98		CBS		
11	23-IM-02	-30	384.46	59.64	6.29	6.28	6.29	BP	C	A	
12	24-IM-02	-30	367.58	47.12	5.75	6.01	5.88	BP	C	A	
13	25-IM-02	-30	*	*	*	*	*	*	*	*	Slippage
14	26-IM-02	-30	312.32	31.31	6.38	6.22	6.30	BP	C	A	
15	54-IM-02	-30	356.19	100.10	6.09	5.88	5.99	BP	C	A	
16	44-IM-02	-30	125.99	63.12	7.01	7.07	7.04		CBS		
17	45-IM-02	-30	204.68	70.60	6.77	7.31	7.04		CBS		
18	27-IM-02	-15	307.54	75.53	6.10	6.26	6.18	BP	C	A	
19	28-IM-02	-15	*	*	*	*	*	*	*	*	Slippage
20	29-IM-02	-15	365.86	60.34	6.40	6.21	6.31	BP	C	A	
21	30-IM-02	-15	428.71	65.51	6.66	6.20	6.43	BP	C	A	
22	46-IM-02	-15	331.80	123.79	6.26	6.22	6.24	BP	C	A	
23	47-IM-02	-15	383.75	130.10	6.73	7.18	6.96		CBS		
24	55-IM-02	-15	333.91	121.37	6.31	6.18	6.25	BP	C	A	
25	60-IM-02	-15	*	*	*	*	*	*	*	*	Slippage
26	31-IM-02	0	432.52	61.10	6.88	6.46	6.67	BP	C	A	
27	32-IM-02	0	405.43	34.55	6.57	6.29	6.43	BP	C	A	
28	33-IM-02	0	361.64	47.62	6.40	6.29	6.35	BP	C	A	
29	48-IM-02	0	317.33	152.76	6.62	6.05	6.34	BP	C	A	
30	49-IM-02	0	299.21	103.40	7.02	6.17	6.60	BP	C	A	
31	56-IM-02	0	363.87	121.81	6.22	6.22	6.22	BP	C	A	
32	59-IM-02	0	314.02	100.31	6.72	6.14	6.43	BP	C	A	
33	9-IM-02	RT	*	*	*	*	*	*	*	*	Slippage
34	10-IM-02	RT	*	*	*	*	*	*	*	*	Slippage
35	11-IM-02	RT	*	*	*	*	*	*	*	*	Slippage
36	12-IM-02	RT	*	*	*	*	*	*	*	*	Slippage
37	13-IM-02	RT	376.95	21.24	7.05	6.47	6.76	BP	C	A	
38	14-IM-02	RT	*	*	*	*	*	*	*	*	Slippage
39	15-IM-02	RT	348.43	57.14	6.34	6.13	6.24	BP	C	A	
40	16-IM-02	RT	454.62	70.99	6.30	6.28	6.29	BP	C	A	
41	36-IM-02	RT	381.22	69.63	6.73	5.88	6.31	BP	C	A	
42	38-IM-02	RT	334.91	44.76	6.91	5.95	6.43	BP	C	A	
43	40-IM-02	RT	315.46	33.21	6.68	6.09	6.39	BP	C	A	

BP: Button pulled; A: DP780-2.0mm; C: DP780-1.2.0mm; CBS: Complete button separation

TABLE C.9: cont'd.

	Specimen	Temp. (ºC)	Energy (J)	Peak Load (kN)	Button Size(mm)			Fracture Mode[6] AWS Standard	Button Separation		Comments
					D_1	D_2	D_{ave}		from	on	
44	57-IM-02	RT	289.14	104.36	7.10	6.47	6.79	BP	C	A	
45	37-IM-02	55	355.74	32.84	6.93	6.63	6.78	BP	C	A	
46	50-IM-02	55	263.21	109.26	7.23	6.72	6.98	BP	C	A	
47	51-IM-02	55	263.54	108.89	6.82	6.69	6.76	BP	C	A	
48	52-IM-02	55	270.88	90.28	6.90	6.60	6.75	BP	C	A	
49	17-IM-02	55	301.89	161.77	6.38	6.40	6.39	BP	C	A	
50	18-IM-02	55	201.47	233.87	6.97	6.44	6.71	BP	C	A	
51	19-IM-02	55	228.02	98.43	6.55	5.98	6.27	BP	C	A	
52	39-IM-02	55	315.69	73.09	7.03	6.26	6.65	BP	C	A	
53	43-IM-02	55	98.80	72.30	6.91	6.63	6.77	BP	C	A	

DP780-2.0mm Sheet clamped on passive pendulum.

BP: Button pulled; A: DP780-2.0mm; C: DP780-1.2.0mm

TABLE C.10: Data Sheet of combination C3: DP780-2.0mm to DP780-1.4mm.

	Specimen	Temp. (ºC)	Energy (J)	Peak Load (kN)	Button Size(mm)			Fracture Mode[6]	Button Separation		Comments
					D_1	D_2	D_{ave}	AWS Standard	from	on	
1	19-IM-03	-60	141.11	67.79	5.61	5.45	5.53	BP	D	A	
2	52-IM-03	-60	251.47	102.48	6.03	7.00	6.52		CBS		
3	54-IM-03	-60	77.81	96.49	7.50	6.66	7.08	BP	A	D	
4	23-IM-03	-60	57.92	31.49	4.96	5.45	5.21	BP	D	A	
5	24-IM-03	-60	96.94	19.86	6.09	7.07	6.58		CBS		
6	41-IM-03	-60	349.99	26.31	6.84	6.76	6.80	FIF			
7	45-IM-03	-60	105.40	80.73	*	*	*	BP	A	D	
8	25-IM-03	-30	82.95	32.72	5.59	5.39	5.49	BP	D	A	
9	26-IM-03	-30	71.49	26.71	5.37	5.55	5.46	BP	D	A	
10	27-IM-03	-30	48.15	33.63	5.75	5.71	5.73	BP	D	A	
11	53-IM-03	-30	102.10	88.54	6.84	7.15	7.00	FIF			
12	58-IM-03	-30	312.64	108.75	6.71	5.90	6.31	BP	D	A	
13	40-IM-03	-30	241.61	54.29	7.07	7.08	7.08	FIF			
14	28-IM-03	-15	132.24	38.68	6.64	6.82	6.73	FIF			
15	29-IM-03	-15	60.34	24.50	6.30	6.57	6.44	FIF			
16	30-IM-03	-15	317.39	42.10	6.29	6.55	6.42	FIF			
17	55-IM-03	-15	155.94	119.16	7.12	6.22	6.67	FIF			
18	39-IM-03	-15	313.40	27.91	6.56	6.61	6.59	FIF			
19	42-IM-03	-15	64.93	42.50	6.50	6.61	6.56	FIF			
20	43-IM-03	-15	379.51	45.65	6.87	7.27	7.07	FIF			
21	46-IM-03	-15	355.10	110.02	5.90	5.73	5.82	BP	D	A	
22	31-IM-03	0	24.64	21.15	6.46	6.13	6.30	FIF			
23	32-IM-03	0	37.19	25.93	6.17	6.63	6.40	FIF			
24	33-IM-03	0	51.37	29.08	6.43	7.06	6.75	FIF			
25	35-IM-03	0	163.44	40.36	6.60	6.73	6.67	FIF			
26	36-IM-03	0	182.68	14.35	6.26	6.63	6.45	FIF			
27	38-IM-03	0	274.92	26.86	6.57	6.66	6.62	FIF			
28	44-IM-03	0	358.30	93.30	6.30	5.79	6.05	BP	D	A	
29	47-IM-03	0	78.89	39.37	7.55	6.33	6.94	BP	D	A	
30	48-IM-03	RT	392.58	129.43	7.25	6.07	6.66	BP	D	A	
31	49-IM-03	RT	312.58	*	7.17	5.99	6.58	BP	D	A	
32	17-IM-03	RT	207.11	86.72	6.42	6.00	6.21	BP	D	A	
33	18-IM-03	RT	214.06	127.46	6.79	6.88	6.84	FIF			
34	16-IM-03	RT	224.48	119.98	6.67	6.61	6.64	FIF			
35	37-IM-03	RT	292.44	82.42	6.73	6.94	6.84	FIF			
36	56-IM-03	RT	73.33	43.13	6.66	6.82	6.74	FIF			
37	57-IM-03	RT	91.10	105.40	6.98	6.74	6.86	FIF			
38	60-IM-03	RT	125.66	27.02	6.80	6.24	6.52	BP	D	A	
39	20-IM-03	55	127.77	55.64	6.88	6.04	6.46	BP	D	A	
40	21-IM-03	55	145.98	80.70	6.75	6.50	6.63	FIF			
41	22-IM-03	55	58.51	31.00	6.37	6.80	6.59	FIF			

DP780-2.0mm Sheet clamped on passive pendulum.
BP: Button pulled; A: DP780-2.0mm; D: DP780-1.4mm;
FIF: Full interfacial fracture; CBS: Complete button separation

TABLE C.10: cont'd.

	Specimen	Temp. (ºC)	Energy (J)	Peak Load (kN)	Button Size(mm)			Fracture Mode[6]	Button Separation		Comments
					D_1	D_2	D_{ave}	AWS Standard	from	on	
42	50-IM-03	55	74.66	*	7.23	6.24	6.74	BP	D	A	
43	51-IM-03	55	107.57	78.51	6.45	6.90	6.68	FIF			
44	34-IM-03	55	113.19	26.91	6.43	6.80	6.62	FIF			
45	59-IM-03	55	80.77	55.71	6.42	5.79	6.11	BP	D	A	

DP780-2.0mm Sheet clamped on passive pendulum.
BP: Button pulled; A: DP780-2.0mm; D: DP780-1.4mm;
FIF: Full interfacial fracture; CBS: Complete button separation

TABLE C.11: Data Sheet of combination C4: DP590-1.0mm to Mild Steel-1.0mm.

	Specimen	Temp.	Energy	Peak Load	Button Size(mm)			Fracture Mode[6]	Button Separation		Comments
		(ºC)	(J)	(kN)	D_1	D_2	D_{ave}	AWS Standard	from	on	
1	32-IM-04	-60	60.69	43.45	7.18	6.92	7.05		CBS		
2	33-IM-04	-60	97.87	64.40	7.15	6.72	6.94	BP	F	E	
3	34-IM-04	-60	123.29	54.16	6.79	7.15	6.97	BP	F	E	A crack extends from the weld to the edge of the sheet
4	46-IM-04	-60	122.04	*	6.93	7.04	6.99	BP	E	F	
5	47-IM-04	-60	108.50	49.42	6.97	7.15	7.06	BP	E	F	
6	55-IM-04	-60	68.82	20.82	6.70	6.88	6.79	BP	E	F	Mild steel splits in two pieces
7	35-IM-04	-30	*	*	*	*	*	*	*	*	Slippage
8	36-IM-04	-30	100.36	32.40	7.06	6.34	6.70	BP	E	F	
9	38-IM-04	-30	176.18	12.42	6.93	7.18	7.06	BP	E	F	
10	39-IM-04	-30	97.50	38.03	7.12	6.91	7.02	BP	E	F	
11	48-IM-04	-30	54.53	77.13	6.89	6.75	6.82	BP	E	F	
12	52-IM-04	-30	*	*	*	*	*	*	*	*	Slippage
13	56-IM-04	-30	*	*	*	*	*	*	*	*	Slippage
14	57-IM-04	-30	*	*	*	*	*	*	*	*	Slippage
15	58-IM-04	-30	55.45	54.42	7.14	7.19	7.17	BP	E	F	
16	37-IM-04	-15	84.20	29.22	6.96	6.64	6.80	BP	E	F	
17	40-IM-04	-15	*	*	*	*	*	*	*	*	Slippage
18	41-IM-04	-15	88.37	18.14	7.03	6.73	6.88	BP	E	F	
19	42-IM-04	-15	69.57	45.25	6.93	6.66	6.80	BP	E	F	
20	59-IM-04	-15	59.23	36.42	7.05	6.55	6.80	BP	E	F	
21	43-IM-04	0	73.89	30.56	6.96	6.75	6.86	BP	E	F	
22	44-IM-04	0	106.57	35.34	6.95	6.80	6.88	BP	E	F	
23	45-IM-04	0	110.79	40.11	6.94	7.19	7.07	BP	E	F	
24	49-IM-04	0	66.17	46.93	6.98	6.93	6.96	BP	E	F	
25	53-IM-04	0	135.21	104.18	7.28	6.58	6.93	BP	E	F	
26	54-IM-04	RT	50.37	100.15	6.92	6.92	6.92	BP	E	F	
27	26-IM-04	RT	118.69	15.50	7.12	6.41	6.77	BP	E	F	
28	27-IM-04	RT	60.34	43.51	7.29	6.95	7.12	BP	E	F	
29	28-IM-04	RT	57.38	25.06	7.16	6.91	7.04	BP	E	F	
30	60-IM-04	RT	*	*	*	*	*	*	*	*	Slippage
31	29-IM-04	55	0.38	22.94	6.30	5.99	6.15	BP	E	F	

Mild steel sheet clamped on passive pendulum.
PB: Button pulled; E: Mild Steel-1mm; F: DP590-1mm; CBS: Complete button separation

TABLE C.11: cont'd.

	Specimen	Temp. (ºC)	Energy (J)	Peak Load (kN)	Button Size(mm)			Fracture Mode[6]	Button Separation		Comments
					D_1	D_2	D_{ave}	AWS Standard	from	on	
32	30-IM-04	55	51.74	32.17	7.12	6.72	6.92	BP	E	F	
33	31-IM-04	55	41.33	39.26	7.01	6.71	6.86	BP	E	F	
34	50-IM-04	55	128.56	19.60	7.06	6.35	6.71	BP	E	F	
35	51-IM-04	55	90.92	38.47	6.57	6.10	6.34	BP	E	F	

Mild steel sheet clamped on passive pendulum.
PB: Button pulled; E: Mild Steel-1mm; F: DP590-1mm; CBS: Complete button separation

TABLE C.12: Data Sheet of combination C5: DP590-1.0mm to Mild Steel- 2.0mm.

	Specimen	Temp.	Energy	Peak Load	Button Size(mm)			Fracture Mode[6]	Button Separation		Comments
		(ºC)	(J)	(kN)	D_1	D_2	D_{ave}	AWS Standard	from	on	
1	22-IM-05	-60	105.01	39.45	6.93	6.75	6.84	BP	G	F	
2	23-IM-05	-60	43.24	29.56	7.19	6.98	7.09		CBS		
3	28-IM-05	-60	136.79	39.42	7.10	6.63	6.87	BP	F	G	
4	38-IM-05	-60	176.10	25.80	6.86	7.16	7.01	BP	F	G	
5	46-IM-05	-60	156.11	91.20	6.48	6.48	6.48	BP	F	G	
6	24-IM-05	-30	172.34	58.77	7.31	7.00	7.16	BP	F	G	
7	25-IM-05	-30	150.52	69.63	6.87	7.08	6.98	BP	F	G	
8	26-IM-05	-30	297.44	96.93	7.30	7.25	7.28	BP	F	G	
9	39-IM-05	-30	168.13	88.62	7.34	7.16	7.25	BP	F	G	
10	47-IM-05	-30	134.71	68.58	7.14	6.55	6.85	BP	F	G	
11	27-IM-05	-15	121.03	51.40	6.98	6.99	6.99	BP	F	G	
12	29-IM-05	-15	307.72	40.25	7.30	6.80	7.05	BP	F	G	
13	30-IM-05	-15	102.70	44.89	*	*	*	*	CBS		
14	40-IM-05	-15	251.16	39.71	7.39	6.98	7.19	BP	F	G	
15	41-IM-05	-15	265.16	14.88	6.49	6.82	6.66	BP	F	G	
16	31-IM-05	0	313.84	54.19	7.07	6.63	6.85	BP	F	G	
17	32-IM-05	0	309.64	70.20	7.29	6.87	7.08	BP	F	G	
18	33-IM-05	0	*	*	*	*	*	*	*	*	Slippage
19	34-IM-05	0	116.48	63.30	6.49	7.04	6.77	BP	F	G	
20	42-IM-05	0	262.84	25.30	6.05	6.84	6.45	BP	F	G	
21	43-IM-05	0	240.80	142.77	6.41	6.79	6.60	BP	F	G	
22	44-IM-05	0	132.55	115.25	7.34	6.22	6.78	BP	G	F	
23	19-IM-05	RT	252.58	106.66	6.58	6.70	6.64	BP	F	G	
24	20-IM-05	RT	288.68	55.97	6.56	6.89	6.73	BP	F	G	
25	21-IM-05	RT	282.67	92.52	6.87	6.87	6.87	BP	F	G	
26	45-IM-05	RT	254.25	79.97	6.22	6.82	6.52	BP	F	G	
27	35-IM-05	55	290.71	74.36	6.45	6.69	6.57	BP	F	G	
28	36-IM-05	55	280.39	73.47	6.24	6.57	6.41	BP	F	G	
29	37-IM-05	55	270.29	41.28	6.20	6.32	6.26	BP	F	G	
30	48-IM-05	55	*	*	*	*	*	*	*	*	Slippage
31	49-IM-05	55	238.59	69.38	6.42	6.90	6.66	BP	F	G	

Mild steel sheet clamped on passive pendulum.

PB: Button pulled; G: Mild Steel-2.0mm; CBS: Complete Button Separation

TABLE C.13: Energy and peak load of combination C1: DP780-2.0mm to DP780-1.0mm, excluding outliers.

	Specimen	Temp. (ºC)	Energy (J)	E_{ave} (J)	Peak Load (kN)	P_{ave} (kN)
1	18-IM-01	-60	247.54		87.06	
2	19-IM-01	-60	216.85		113.81	
3	30-IM-01	-60	646.66		29.04	
4	53-IM-01	-60	53.05		26.31	
5	55-IM-01	-60	259.15	176.59	48.01	60.85
6	31-IM-01	-30	317.61		84.97	
7	32-IM-01	-30	270.00		98.72	
8	33-IM-01	-30	60.34		54.62	
9	49-IM-01	-30	53.82		*	
10	58-IM-01	-30	252.61	190.88	25.21	65.88
11	50-IM-01	-15	147.59		111.53	
12	59-IM-01	-15	130.37		81.74	
13	56-IM-01	-15	263.42	180.46	95.67	96.31
14	39-IM-01	0	35.82		25.49	
15	47-IM-01	0	58.09		47.26	
16	48-IM-01	0	50.33		54.32	
17	51-IM-01	0	57.63		*	
18	60-IM-01	0	34.64	47.30	5.13	33.05
19	24-IM-01	RT	336.26		*	
20	21-IM-01	RT	135.61		63.79	
21	23-IM-01	RT	243.73		105.19	
22	52-IM-01	RT	54.52		65.34	
23	54-IM-01	RT	62.17	166.46	36.80	67.78
24	26-IM-01	55	70.20		*	
25	27-IM-01	55	118.76		*	
26	41-IM-01	55	63.69		28.34	
27	44-IM-01	55	85.65	84.58	23.82	26.08

TABLE C.14: Energy and peak load for specimens w/ expulsion of combination C1: DP780-2.0mm to DP780-1.0mm, excluding the outlier.

	Specimen	Temp. (°C)	Energy (J)	E_{ave} (J)	Peak Load (kN)	P_{ave} (kN)
1	53-IM-01	-60	53.05	53.05	26.31	26.31
2	33-IM-01	-30	60.34		54.62	
3	49-IM-01	-30	53.82	57.08	*	54.62
4	59-IM-01	-15	130.37		81.74	
5	37-IM-01	-15	62.27		25.01	
6	45-IM-01	-15	52.78		23.61	
7	46-IM-01	-15	47.72	73.29	30.44	40.20
8	60-IM-01	0	34.64		5.13	
9	39-IM-01	0	35.82		25.49	
10	48-IM-01	0	50.33	40.26	54.32	28.32
11	54-IM-01	RT	62.17		36.80	
12	52-IM-01	RT	54.52	58.34	65.34	51.07
13	26-IM-01	55	70.20		*	
14	41-IM-01	55	63.69		28.34	
15	42-IM-01	55	41.43		37.66	
16	44-IM-01	55	85.65	65.24	23.82	29.94

TABLE C.15: Energy and peak load for specimens w/o expulsion of combination C1: DP780-2.0mm to DP780-1.0mm, excluding the outlier.

	Specimen	Temp. (^oC)	Energy (J)	E_{ave} (J)	Peak Load (kN)	P_{ave} (kN)
1	55-IM-01	-60	259.15		48.01	
2	18-IM-01	-60	247.54		87.06	
3	19-IM-01	-60	216.85	241.18	113.81	82.96
4	58-IM-01	-30	252.61		25.21	
5	31-IM-01	-30	317.61		84.97	
6	32-IM-01	-30	270.00	280.08	98.72	69.63
7	56-IM-01	-15	263.42		95.67	
8	34-IM-01	-15	354.06		73.74	
9	36-IM-01	-15	292.90		43.49	
10	50-IM-01	-15	147.59	264.49	111.53	81.11
11	38-IM-01	0	317.42		86.45	
12	40-IM-01	0	289.88	303.65	36.89	61.67
13	24-IM-01	RT	336.26		*	
14	22-IM-01	RT	368.19		83.23	
15	23-IM-01	RT	243.73	316.06	105.19	94.21
16	25-IM-01	55	289.46		84.19	
17	28-IM-01	55	323.97		56.02	
18	29-IM-01	55	334.50	315.98	50.25	63.49

TableC.16: Average energy and peak load of combination C1: DP780-2.0mm to DP780-1.0mm w/ and w/o expulsion.

Temp. (ºC)	Energy (J)		Peak Load (kN)	
	w/Expulsion	w/o Expulsion	w/Expulsion	w/o Expulsion
-60	53.05	241.18	26.31	82.96
-30	57.08	280.08	54.62	69.63
-15	73.29	264.49	40.20	81.11
0	40.26	303.65	28.32	61.67
30	58.34	316.06	51.07	94.21
55	65.24	315.98	29.94	63.49

TABLE C.17: Energy and peak load of combination C2: DP780-2.0mm to DP780-1.2.0mm, excluding outliers.

	Specimen	Temp. (ºC)	Energy (J)	E_{ave} (J)	Peak Load (kN)	P_{ave} (kN)
1	21-IM-02	-60	398.67		65.82	
2	34-IM-02	-60	337.75		73.85	
3	42-IM-02	-60	346.16	360.86	92.35	77.34
4	23-IM-02	-30	384.46		59.64	
5	24-IM-02	-30	367.58		47.12	
6	26-IM-02	-30	312.32		31.31	
7	45-IM-02	-30	204.68		70.60	
8	54-IM-02	-30	356.19	325.05	100.10	61.75
9	29-IM-02	-15	365.86		60.34	
10	46-IM-02	-15	331.80		123.79	
11	47-IM-02	-15	383.75		130.10	
12	55-IM-02	-15	333.91	353.83	121.37	108.90
13	32-IM-02	0	405.43		34.55	
14	33-IM-02	0	361.64		47.62	
15	48-IM-02	0	317.33		152.76	
16	56-IM-02	0	363.87		121.81	
17	59-IM-02	0	314.02	352.46	100.31	91.41
18	13-IM-02	RT	376.95		21.24	
19	15-IM-02	RT	348.43		57.14	
20	36-IM-02	RT	381.22		69.63	
21	38-IM-02	RT	334.91		44.76	
22	40-IM-02	RT	315.46	351.39	33.21	45.20
23	17-IM-02	55	301.89		161.77	
24	18-IM-02	55	201.47		233.87	
25	19-IM-02	55	228.02		98.43	
26	39-IM-02	55	315.69		73.09	
27	50-IM-02	55	263.21		109.26	
28	51-IM-02	55	263.54		108.89	
29	52-IM-02	55	270.88	263.53	90.28	125.08

TABLE C.18: Energy and peak load of combination C3: DP780-2.0mm to DP780-1.4mm, excluding the outliers.

	Specimen	Temp. (°C)	Energy (J)	E_{ave} (J)	Peak Load (kN)	P_{ave} (kN)
1	19-IM-03	-60	141.11		67.79	
2	23-IM-03	-60	57.92		31.49	
3	24-IM-03	-60	96.94		19.86	
4	45-IM-03	-60	105.40		80.73	
5	52-IM-03	-60	251.47		102.48	
6	54-IM-03	-60	77.81	121.77	96.49	66.47
7	25-IM-03	-30	82.95		32.72	
8	26-IM-03	-30	71.49		26.71	
9	27-IM-03	-30	48.15		33.63	
10	40-IM-03	-30	241.61		54.29	
11	53-IM-03	-30	102.10	109.26	88.54	47.18
12	28-IM-03	-15	132.24		38.68	
13	30-IM-03	-15	317.39		42.10	
14	39-IM-03	-15	313.40		27.91	
15	55-IM-03	-15	155.94	229.74	119.16	56.97
16	33-IM-03	0	51.37		29.08	
17	35-IM-03	0	163.44		40.36	
18	36-IM-03	0	182.68		14.35	
19	47-IM-03	0	78.89	119.09	39.37	30.79
20	16-IM-03	RT	224.48		119.98	
21	17-IM-03	RT	207.11		86.72	
22	18-IM-03	RT	214.06		127.46	
23	37-IM-03	RT	292.44	234.52	82.42	104.14
24	20-IM-03	55	127.77		55.64	
25	34-IM-03	55	113.19		26.91	
26	50-IM-03	55	74.66		*	
27	51-IM-03	55	107.57		78.51	
28	59-IM-03	55	80.77	100.79	55.71	54.19

TABLE C.19: Energy and peak load for specimens w/ interfacial fracture of combination C3: DP780-2.0mm to DP780-1.4mm.

	Specimen	Temp. (ºC)	Energy (J)	E_{ave} (J)	Peak Load (kN)	P_{ave} (kN)
1	41-IM-03	-60	349.99	349.99	26.31	26.31
2	40-IM-03	-30	241.61		54.29	
3	53-IM-03	-30	102.10	171.86	88.54	71.42
4	28-IM-03	-15	132.24		38.68	
5	29-IM-03	-15	60.34		24.50	
6	30-IM-03	-15	317.39		42.10	
7	39-IM-03	-15	313.40		27.91	
8	42-IM-03	-15	64.93		42.50	
9	43-IM-03	-15	379.51		45.65	
10	55-IM-03	-15	155.94	203.39	119.16	48.64
11	31-IM-03	0	24.64		21.15	
12	32-IM-03	0	37.19		25.93	
13	33-IM-03	0	51.37		29.08	
14	35-IM-03	0	163.44		40.36	
15	36-IM-03	0	182.68		14.35	
16	38-IM-03	0	274.92	122.37	26.86	26.29
17	16-IM-03	RT	224.48		119.98	
18	18-IM-03	RT	214.06		127.46	
19	37-IM-03	RT	292.44		82.42	
20	56-IM-03	RT	73.33		43.13	
21	57-IM-03	RT	91.10	179.08	105.40	95.68
22	21-IM-03	55	145.98		80.70	
23	22-IM-03	55	58.51		31.00	
24	34-IM-03	55	113.19		26.91	
25	51-IM-03	55	107.57	106.31	78.51	54.28

TABLE C.20: Energy and peak load for specimens w/o interfacial fracture of combination C3: DP780-2.0mm to DP780-1.4mm.

	Specimen	Temp. (ºC)	Energy (J)	E_{ave} (J)	Peak Load (kN)	P_{ave} (kN)
1	23-IM-03	-60	57.92		31.49	
2	19-IM-03	-60	141.11		67.79	
3	24-IM-03	-60	96.94		19.86	
4	45-IM-03	-60	105.40		80.73	
5	52-IM-03	-60	251.47		102.48	
6	54-IM-03	-60	77.81	121.77	96.49	66.47
7	25-IM-03	-30	82.95		32.72	
8	26-IM-03	-30	71.49		26.71	
9	27-IM-03	-30	48.15		33.63	
10	58-IM-03	-30	312.64	128.81	108.75	50.45
11	46-IM-03	-15	355.10	355.10	110.02	110.02
12	44-IM-03	0	358.30		93.30	
13	47-IM-03	0	78.89	218.60	39.37	66.33
14	17-IM-03	RT	207.11		86.72	
15	48-IM-03	RT	392.58		129.43	
16	49-IM-03	RT	312.58		*	
17	60-IM-03	RT	125.66	259.48	27.02	81.06
18	20-IM-03	55	127.77		55.64	
19	50-IM-03	55	74.66		*	
20	59-IM-03	55	80.77	94.40	55.71	55.67

TableC.21: Average energy and peak load of combination C3: DP780-2.0mm to DP780-1.4mm w/ and w/o interfacial fracture.

Temp. (ºC)	Energy (J)		Peak Load (kN)	
	w/Interfacial fracture	w/o Interfacial fracture	w/Interfacial fracture	w/o Interfacial fracture
-60	349.99	121.77	26.31	66.47
-30	171.86	128.81	71.42	50.45
-15	203.39	355.10	48.64	110.02
0	122.37	218.60	26.29	66.33
30	179.08	259.48	95.68	81.06
55	106.31	94.40	54.28	55.67

TABLE C.22: Energy and peak load of combination C4: DP590-1.0mm to Mild Steel-1.0mm.

	Specimen	Temp. (ºC)	Energy (J)	E_{ave} (J)	Peak Load (kN)	P_{ave} (kN)
1	33-IM-04	-60	97.87		64.40	
2	34-IM-04	-60	123.29		54.16	
3	46-IM-04	-60	122.04		*	
4	47-IM-04	-60	108.50		49.42	
5	55-IM-04	-60	68.82	104.10	20.82	47.20
6	36-IM-04	-30	100.36		32.40	
7	39-IM-04	-30	97.50		38.03	
8	48-IM-04	-30	54.53		77.13	
9	58-IM-04	-30	55.45	76.96	54.42	50.49
10	37-IM-04	-15	84.20		29.22	
11	41-IM-04	-15	88.37		18.14	
12	42-IM-04	-15	69.57		45.25	
13	59-IM-04	-15	59.23	75.34	36.42	32.26
14	43-IM-04	0	73.89		30.56	
15	44-IM-04	0	106.57		35.34	
16	45-IM-04	0	110.79		40.11	
17	49-IM-04	0	66.17	89.35	46.93	38.24
18	26-IM-04	RT	118.69		15.50	
19	27-IM-04	RT	60.34		43.51	
20	28-IM-04	RT	57.38		25.06	
21	54-IM-04	RT	50.37	71.70	100.15	46.06
22	30-IM-04	55	51.74		32.17	
23	31-IM-04	55	41.33		39.26	
24	51-IM-04	55	90.92	61.33	38.47	36.64

TABLE C.23: Energy and peak load of combination C5: DP590-1.0mm to Mild Steel-2.0mm.

	Specimen	Temp. (ºC)	Energy (J)	E_{ave} (J)	Peak Load (kN)	P_{ave} (kN)
1	22-IM-05	-60	105.01		39.45	
2	28-IM-05	-60	136.79		39.42	
3	38-IM-05	-60	176.10		25.80	
4	46-IM-05	-60	156.11	143.50	91.20	48.97
5	24-IM-05	-30	172.34		58.77	
6	25-IM-05	-30	150.52		69.63	
7	39-IM-05	-30	168.13		88.62	
8	47-IM-05	-30	134.71	156.42	68.58	71.40
9	27-IM-05	-15	121.03		51.40	
10	29-IM-05	-15	307.72		40.25	
11	30-IM-05	-15	102.70		44.89	
12	40-IM-05	-15	251.16		39.71	
13	41-IM-05	-15	265.16	209.56	14.88	38.23
14	31-IM-05	0	313.84		54.19	
15	32-IM-05	0	309.64		70.20	
16	42-IM-05	0	262.84		25.30	
17	43-IM-05	0	240.80	281.78	142.77	73.12
18	19-IM-05	RT	252.58		106.66	
19	20-IM-05	RT	288.68		55.97	
20	21-IM-05	RT	282.67		92.52	
21	45-IM-05	RT	254.25	269.55	79.97	83.78
22	35-IM-05	55	290.71		74.36	
23	36-IM-05	55	280.39		73.47	
24	37-IM-05	55	270.29		41.28	
25	49-IM-05	55	238.59	270.00	69.38	64.62

Auto/Steel Partnership

2000 Town Center, Suite 320
Southfield, Michigan 48075
Tel: 248.945.4777
www.a-sp.org

The New Steel